LIFE SCIENCES

The myokine irisin ameliorates the secretory dysfunction of pancreatic β cells in experimental and human type 2 diabetes

Nicola Marrano[1]†, Anna Borrelli[1]†, Giuseppina Biondi[1], Martina Rella[1], Rossella D'Oria[1], Valentina Annamaria Genchi[1], Cristina Caccioppoli[1], Valerio Galasso[1], Giovanni Galluzzi[1], Luca Roberto[2], Anna Signorile[3], Leonardo Vincenti[4], Fabrizio Aquilino[4], Rita Nano[5], Federico Baruzzi[6], Antonio Moretti[6], Luigi Giovanni Lupo[7], Piero Marchetti[8], Lorenzo Piemonti[5], Angelo Cignarelli[1], Sebastio Perrini[1,9], Luigi Laviola[1], Francesco Giorgino[1]*, Annalisa Natalicchio[1]

Irisin is a myokine that enhances insulin secretion and β cell viability in both rodent and human β cells. Here, we investigated whether irisin preserves β cell functional mass in vivo in diabetic mice and ex vivo in human pancreatic islets from subjects with type 2 diabetes (T2D). In mice made diabetic by a high-fat diet and streptozotocin, irisin administration improved glycemic homeostasis by increasing islet insulin content and glucose-stimulated insulin secretion while also markedly stimulating β cell proliferation. In islets from T2D subjects, which typically display substantial structural and functional impairments, irisin restored insulin content and glucose-stimulated insulin secretion. Mechanistic studies in INS-1E cells showed that chronic exposure to high glucose blunted glucose-triggered cytoplasmic calcium increases, essential for insulin secretion. Under these glucotoxic conditions, while irisin was unable to activate CREB and AKT, it induced AMPK-mTORC1-S6K–dependent mobilization of endoplasmic reticulum calcium stores, resulting in enhancement of insulin secretion. Overall, these findings highlight irisin's multifaceted ability to counteract β cell failure in experimental and human T2D.

INTRODUCTION

The loss of functional β cell mass is an essential and early event in the development of type 2 diabetes (T2D) (*1*). At the time of diagnosis, β cell function is already significantly impaired in individuals with T2D and continues to deteriorate progressively (*2*, *3*). In addition, β cell mass itself is reduced in patients with T2D, with studies reporting reductions ranging from ~20 to 65%, and pancreatic islets from diabetic donors show structural changes compared to those from nondiabetic donors (*4*–*6*). Thus, strategies aimed at regenerating β cells or preserving the functional integrity of islets are critical avenues to explore for the effective treatment and potential cure of T2D (*1*). Current antidiabetic medications have been conceived to primarily lower elevated blood glucose levels, without necessarily addressing the underlying pathology (*7*). A truly effective antidiabetic therapy should ideally prevent β cell loss and facilitate restoration or regeneration of a fully functional β cell mass (*1*).

Irisin, a 112-aminoacid peptide, resulting from the proteolytic cleavage of the extracellular N-terminal portion of the membrane protein fibronectin type III domain containing protein 5, was first identified as a myokine released following physical activity and driving brown fat-like development of white adipose tissue and thermogenesis (*8*). Numerous studies have subsequently documented the pivotal role of irisin in the regulation of energy metabolism, by promoting glucose uptake and utilization/storage in skeletal muscle and adipose tissue and reducing hepatic glucose production (*9*). Notably, a dysregulation of irisin secretion or action has been associated with several pathological conditions, such as T2D, obesity, cardiovascular diseases, osteoporosis/fractures, muscle atrophy, neurodegenerative diseases, and cancer (*9*, *10*). When focusing on dysmetabolic states, however, the evidence remains partly inconsistent. In individuals with prediabetes or at early stages of dysglycemia, most studies report increased circulating irisin levels and positive association with obesity, insulin resistance, and markers of adiposity (*11*–*16*), possibly reflecting a compensatory response. Conversely, other studies have described reduced irisin concentrations in similar populations, with either no significant or even inverse correlations with metabolic parameters (*17*–*19*). In contrast, decreased circulating irisin levels in overt T2D have been more consistently reported across studies, including relevant meta-analyses (*12*, *13*, *20*–*22*).

We have previously demonstrated that irisin exerts significant insulin secretagogue and prosurvival effects in pancreatic islets (*23*). Irisin enhances insulin content and secretion, in a cyclic adenosine 3′,5′-monophosphate (cAMP)–dependent protein kinase (PKA)/cAMP response element–binding protein (CREB)–dependent manner, protects pancreatic islets from fatty acid–induced apoptosis, through a mechanism involving the activation of AKT/Bcl-2 antiapoptotic signaling (*23*), and promotes β cell proliferation through the activation of the extracellular signal–regulated kinase 1/2 (ERK1/2) pathway (*24*). In addition, when administered in vivo, irisin improves glucose-stimulated insulin secretion (GSIS) and increases insulin content, β cell mass, and proliferation in nondiabetic nonobese mice (*23*).

[1]Department of Precision and Regenerative Medicine and Ionian Area, Section of Internal Medicine, Endocrinology, Andrology and Metabolic Diseases, University of Bari Aldo Moro, Bari, Italy. [2]Transgenic Mice Facility, Biogem S.c.ar.l., Ariano Irpino, Avellino, Italy. [3]Department of Translational Biomedicine and Neuroscience, University of Bari Aldo Moro, Bari, Italy. [4]General Surgery Unit, National Institute of Gastroenterology "Saverio de Bellis," Research Hospital, Castellana Grotte, Bari, Italy. [5]Diabetes Research Institute, IRCCS San Raffaele Hospital, Milan, Italy. [6]Institute of Sciences of Food Production, National Research Council of Italy, (CNR-ISPA), Bari, Italy. [7]Department of Precision and Regenerative Medicine and Ionian Area, Section of General Surgery and Liver Transplantation, University of Bari Aldo Moro, Bari, Italy. [8]Department of Clinical and Experimental Medicine, University of Pisa, Pisa, Italy. [9]Department of Medicine and Surgery, Section of Endocrinology, LUM University, Casamassima, Bari, Italy.
*Corresponding author. Email: francesco.giorgino@uniba.it
†These authors contributed equally to this work.

Stimulation of insulin secretion by irisin is observed only in the presence of high glucose, which can minimize the risk of hypoglycemia (*23*). Other studies have similarly shown that irisin can increase the proliferation of rat insulinoma-derived insulin–secreting (INS)–1 cells via ERK and p38 mitogen-activated protein kinase, protect these cells from glucotoxicity-induced apoptosis, and improve pancreatic β cell function in a rat model of T2D (*24*). Furthermore, in INS-1E cells and islets isolated from C57BL/6 mice and then exposed to glucolipotoxic conditions, irisin enhances the expression of genes related to β cell survival and function via AMP-activated protein kinase (AMPK)–mediated suppression of lipogenic gene expression and the consequent reduction in intracellular fatty acids/triglycerides (*25*). More recently, multiple studies have also demonstrated that irisin attenuates β cell pyroptosis both in vitro and in vivo in mouse model of T2D (*26*–*30*).

In this study, we address the therapeutic potential of irisin by describing its effects on the β cell functional mass in a mouse model of T2D in vivo and in human pancreatic islets isolated from subjects with T2D ex vivo. We also hypothesize that irisin restores β cell function under dysmetabolic conditions by modulating AMPK–mechanistic target of rapamycin complex 1 (mTORC1) signaling, and endoplasmic reticulum (ER) calcium dynamics. Dysregulation of the AMPK-mTORC1 pathway has been implicated in β cell dysfunction induced by chronic hyperglycemia (*31*). Specifically, glucotoxicity inhibits AMPK phosphorylation, leading to sustained mTORC1 hyperactivation and increased signaling through its downstream effector, ribosomal protein S6 kinase (S6K). This aberrant activation contributes to impaired insulin secretion and progressive β cell failure (*31*, *32*). Evidence from other systems suggests that irisin can activate AMPK in various disease models, including diabetes (*33*). Notably, AMPK also mediates the ability of irisin to modulate ER calcium release in vascular smooth muscle cells (*34*). Conversely, GSIS in pancreatic β cells can be enhanced by glucagon-like peptide-1 (GLP-1), a hormone that shares several signaling pathways with irisin (*9*), partly through mobilization of intracellular calcium from the ER (*35*). These observations provide a rationale for investigating whether irisin may influence β cell function through coordinated regulation of AMPK-mTORC1-S6K signaling and ER calcium mobilization.

RESULTS

The in vivo administration of irisin ameliorates hyperglycemia and reduces excess body weight in a mouse model of T2D

We first studied the effects of in vivo administration of irisin in a mouse model of T2D induced by a high-fat diet (HFD) combined with a single low-dose streptozotocin (STZ) injection. We then divided diabetic mice into two groups with equal metabolic characteristics at baseline (table S1) and injected them daily via the intraperitoneal route with irisin (0.5 μg/g) or vehicle for 14 days. Standard diet (SD)–fed mice served as control (fig. S1A). Compared to control mice, diabetic mice showed higher body weight (Fig. 1A) and fasting glycemia (Fig. 1B), with a trend of decreasing fasting insulinemia (Fig. 1C). Irisin administration significantly reduced body weight (Fig. 1A) without inducing changes in food intake (Fig. 1D), reduced elevated fasting glycemia to almost nondiabetic levels (Fig. 1B), and increased fasting insulin levels (Fig. 1C). In addition, on the last day of the study protocol, we performed an intraperitoneal glucose tolerance test (IPGTT). Compared to control mice, diabetic mice showed a greater increase in blood glucose levels after the glucose challenge and failed to return to baseline levels even after 3 hours (Fig. 1, E and F). Irisin administration improved glucose tolerance in the diabetic mice (Fig. 1E) and reduced the glucose area under the curve (AUC; Fig. 1F). Diabetic mice were also characterized by reduced insulin secretion and insulin AUC after the glucose challenge, while irisin administration markedly augmented these parameters (Fig. 1, G and H). To minimize the influence of basal insulin levels and specifically assess GSIS, we additionally calculated the incremental insulin AUC over the (0 to 15)–minute interval. Within this early time frame, the differences between control and diabetic mice were no longer evident; nevertheless, irisin administration significantly increased GSIS (fig. S1B). On the other hand, insulin sensitivity, as evaluated by the Matsuda index, was reduced in diabetic mice compared to control mice and was not restored by irisin administration (fig. S1C). Similarly, using the homeostatic model assessment of insulin resistance (HOMA-IR) index, there was a trend to reduced insulin sensitivity in diabetic mice, and this was not modified by irisin (fig. S1D). In addition, irisin administration to diabetic mice up-regulated the mRNA expression levels of browning-related genes, such as uncoupling protein 1 (*Ucp1*), peroxisome proliferative activated receptor γ coactivator-α (*Ppargca1a*), and positive regulatory domain containing 16 (*Prdm16*), in gonadal adipose tissue (fig. S1, E to G, and Supplementary Materials and Methods). Together, these results show that the in vivo administration of irisin to a mouse model of T2D ameliorates hyperglycemia by increasing GSIS.

The in vivo administration of irisin restores pancreatic islet architecture in diabetic mice

We next assessed the effects of irisin on pancreatic islet architecture in vivo, β and α cell area, insulin content, β cell proliferation, and apoptosis levels. In the absence of changes in pancreas weight (Fig. 2A), islets from diabetic mice showed reduced islet mean area (Fig. 2, B and C) and β cell area (Fig. 2, B and D), increased α cell area (Fig. 2, B and E), and reduced insulin content (Fig. 2, B and F) compared to controls. Irisin treatment fully reversed these changes (Fig. 2, B to F). Although apoptosis is thought to be a major contributor to loss of β cells mass, we did not detect apoptotic β cells in any of the analyzed sections and experimental groups (Fig. 2G and fig. S2A). Irisin treatment of diabetic mice resulted in a marked increase in β cell proliferation (9-fold and 4.5-fold compared to control and vehicle-treated diabetic mice, respectively; Fig. 2, H and I). We also observed a slight increase in cell proliferation in the exocrine pancreas, although this was similar in diabetic mice treated with vehicle or irisin compared to control mice and could be due to HFD (fig. S2, B and C). These images replicate those in Fig. 2H; however, in this case, we analyzed nonislet cells. Together, these data indicate that the in vivo administration of irisin to diabetic mice with reduced β cell functional mass restores pancreatic islet architecture by promoting β cell proliferation and increasing β cell area.

Irisin restores GSIS and calcium signaling through an AMPK-dependent mechanism in INS-1E cells and murine islets exposed to glucotoxic conditions

To gain insight into irisin signaling in β cells under dysmetabolic conditions, we investigated its effects in INS-1E cells cultured under control conditions and in the presence of excess chronic glucose. While irisin was able to phosphorylate both CREB (Fig. 3, A and B) and AKT (Fig. 3, A and C) under control conditions, these effects were lost under glucotoxic conditions (Fig. 3, A to C). Furthermore,

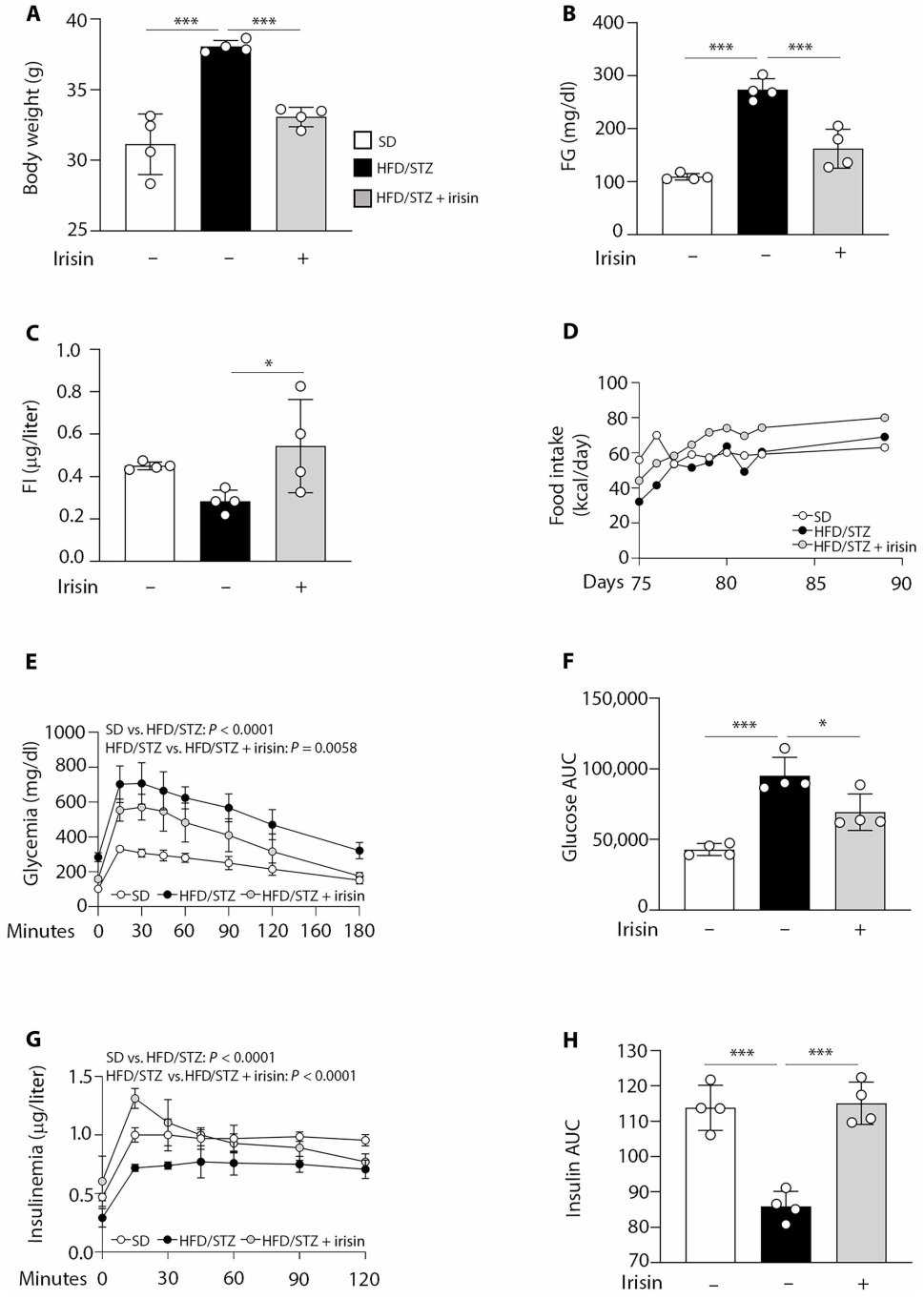

Fig. 1. Irisin improves glycemic homeostasis and reduces excess body weight in a mouse model of T2D. Six-week-old male C57Bl/6J mice ($n = 8$) were fed a HFD for 89 days and intraperitoneally injected with STZ (100 mg/kg) on day 64. Starting on day 75, HFD/STZ mice were intraperitoneally injected with irisin (0.5 µg/g; $n = 4$) or vehicle ($n = 4$), daily for 14 days. SD-fed mice ($n = 4$) served as control. (**A**) Body weight on day 89 is shown ($n = 4$ mice per experimental group). (**B**) Fasting glycemia (FG) and (**C**) fasting insulinemia (FI) on day 89 are shown ($n = 4$ mice per experimental group). (**D**) Starting from the time of irisin administration, food intake was recorded daily by subtracting the amount of feed leftovers from the daily amount given ($n = 4$ mice per experimental group). (**E** to **H**) On day 89, an IPGTT was performed: Mice were intraperitoneally injected with 20% glucose (2 g glucose/kg body weight), and serum and plasma were collected immediately before and 15, 30, 45, 60, 90, 120, and 180 min after glucose injection. (E) Glucose levels measured during IPGTT and (F) AUC of (E) ($n = 4$ mice per experimental group). (G) Insulin levels measured during IPGTT and (H) AUC of (G) ($n = 4$ mice per experimental group). Data are represented as mean ± SD; $^*P < 0.05$ and $^{***}P < 0.001$. (A to C, F, and H) Statistical test was one-way analysis of variance (ANOVA) with Sidak's post hoc test. (D, E, and G) Statistical test was two-way ANOVA with Tukey's post hoc tests.

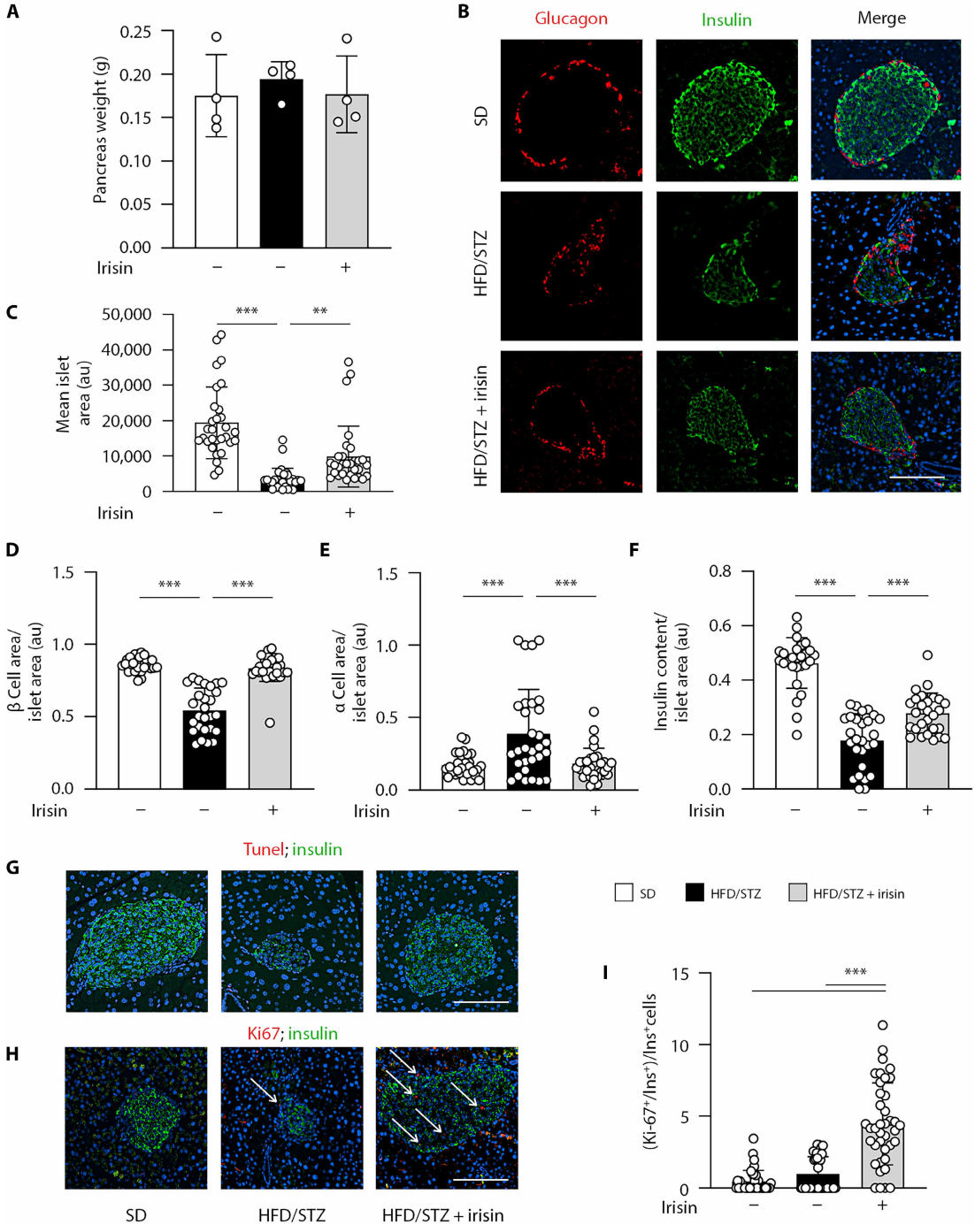

Fig. 2. Irisin restores pancreatic islet architecture in a mouse model of T2D. (**A**) Pancreas weight expressed in grams in SD-fed, HFD/STZ, and irisin-treated HFD/STZ mice ($n = 4$ mice per experimental group). (**B**) Representative immunofluorescence images of pancreas sections. Sections were immunostained for insulin (green) and glucagon (red). Nuclear staining was with 4′,6-diamidino-2-phenylindole (DAPI; blue). Scale bar, 100 μm. (**C**) Islet area measurement was performed with ImageJ software, using the freehand selections and the measure tools ($n = 30$ islets from four mice per experimental group). (**D**) β Cell area was measured using the CellProfiler software as insulin-positive cell area and normalized against total islet area ($n = 27$ islets from four mice per experimental group). (**E**) α Cell area was measured using the CellProfiler software as glucagon-positive cell area and normalized against total islet area ($n = 30$ islets from four mice per experimental group). (**F**) Insulin content was measured using the CellProfiler software as intensity of green staining and normalized against total islet area ($n = 27$ islets from four mice per experimental group). (**G**) Representative immunofluorescence images of pancreas sections. Sections were immunostained for insulin (green) and terminal deoxynucleotidyl transferase–mediated deoxyuridine triphosphate nick end labeling reagents (red). Nuclear staining was with DAPI (blue). Scale bar, 100 μm. (**H**) Representative immunofluorescence images of pancreas sections. Sections were immunostained for insulin (green) and Ki-67 (red). Nuclear staining was with DAPI (blue). Scale bar, 100 μm. (**I**) Cells double positive to insulin/Ki-67 staining, measured using the CellProfiler software, were considered proliferating β cells ($n = 39$ islets from four mice per experimental group). Data are represented as mean ± SD; $^{**}P < 0.01$ and $^{***}P < 0.001$. Statistical test was one-way ANOVA with Sidak's post hoc test. au, arbitrary units; Ins, insulin.

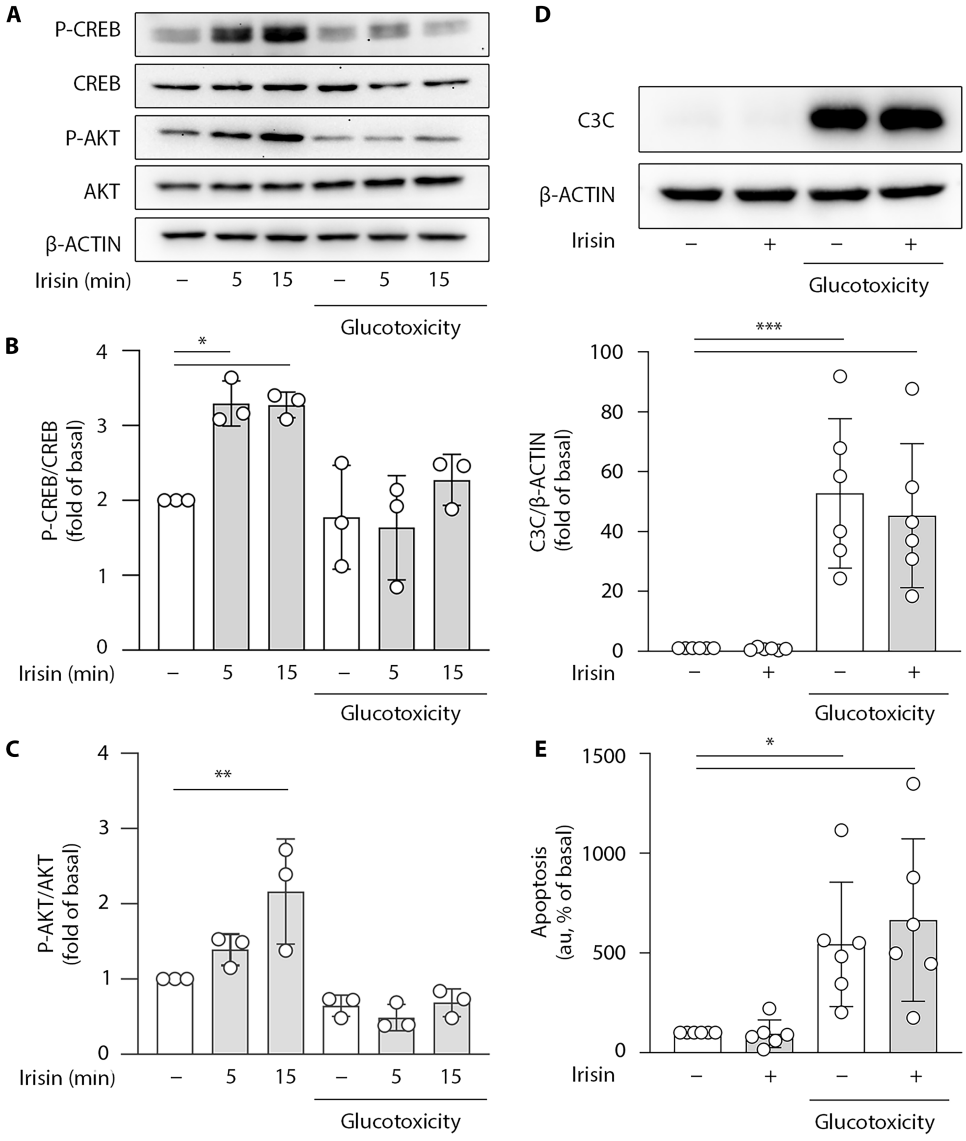

Fig. 3. Irisin does not activate AKT/CREB signaling or affect apoptosis in INS-1E cells under glucotoxicity. (**A** to **C**) INS-1E cells were cultured under glucotoxic conditions (25 mM glucose) for 24 hours to mimic hyperglycemia and then treated with 100 nM irisin at the indicated times. Protein lysates were subjected to immunoblot analysis. (A) Representative immunoblot images. Densitometric analysis of (B) P-CREB and (C) P-AKT bands, expressed as relative optical density, corrected using (B) total CREB or (C) total AKT, and normalized against untreated control ($n = 3$ independent experiments). (**D** and **E**) INS-1E cells were cultured under glucotoxic conditions (25 mM glucose) for 24 hours to mimic hyperglycemia and then treated with 100 nM irisin for 24 hours. (D) Apoptosis levels evaluated by immunoblotting against cleaved caspase-3 (CC3). Top: representative immunoblot images. Bottom: densitometric analysis of the related bands, expressed as relative optical density, corrected using β-actin, and normalized against untreated control ($n = 6$ independent experiments). (E) Apoptosis levels evaluated by measuring cytoplasmic oligonucleosomes with an enzyme-linked immunosorbent assay (ELISA) assay. Data are expressed as percent of basal ($n = 6$ independent experiments). Data are represented as mean ± SD; $^{*}P < 0.05$, $^{**}P < 0.01$, and $^{***}P < 0.001$. Statistical test was one-way ANOVA with Sidak's post hoc test.

apoptosis induced by glucotoxic condition was not reduced by subsequent irisin treatment (Fig. 3, D and E). These results indicate that in the presence of glucotoxicity, irisin signaling via CREB and AKT and its antiapoptotic effect are abrogated.

Besides apoptosis, because in vivo administration of irisin to diabetic mice enhances insulin secretion (Fig. 1), we investigated the effects of irisin on GSIS and calcium flux, a key event in insulin secretion, in INS-1E cells exposed to glucotoxic conditions. In the presence of glucotoxicity, the acute glucose-induced increase in cytosolic calcium levels was markedly blunted; however, following treatment with irisin for 1 hour, this response was fully restored (Fig. 4A). The lack of increase in cytosolic calcium levels after acute glucose challenge under glucotoxic conditions may depend on two primary reasons. First, calcium levels may be basally elevated, attenuating the further increase in cytosolic calcium levels in response to acute secretory stimuli (*36*). However, in our experiments, glucotoxicity increased basal cytosolic calcium levels only after 48 hours, while at 24 hours they were unchanged (fig. S3A). Second, glucotoxicity could reduce the protein expression of the L-type voltage-gated calcium channel (L-VGCC) alpha 1C subunit (Cav1.2), which mediates

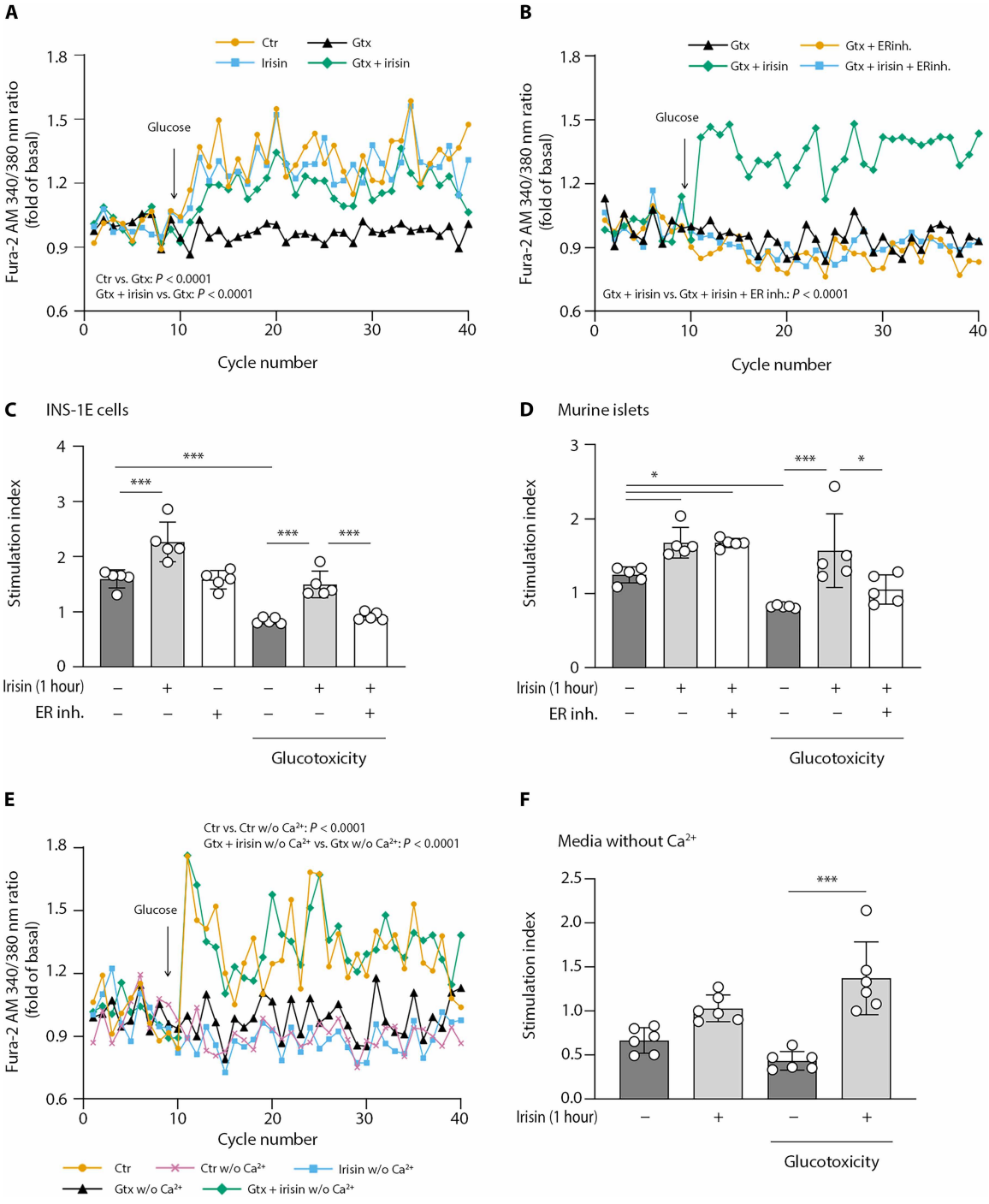

Fig. 4. Irisin restores calcium signaling and GSIS in INS-1E cells and murine islets under glucotoxicity. (**A**) INS-1E cells were cultured for 24 hours under glucotoxic (Gtx; 25 mM glucose) or control glucose (11 mM) conditions and subsequently treated with 100 nM irisin for 1 hour or left untreated. Cells were then sequentially incubated in low (3 mM) and high (25 mM) glucose KRBH buffer. Intracellular calcium was measured using 1 μM Fura-2 AM fluorescence calcium reporter, and fluorescence was recorded for 10 cycles before and 30 cycles after 25 mM acute-glucose stimulation. Data are expressed as the 340/380-nm fluorescence ratio and presented as fold of basal fluorescence ($n = 12$ independent experiments). (**B**) Calcium fluxes were assessed as in (A), with or without pretreatment (30 min) with ER calcium receptor inhibitors (ER inh., 1 μM xestospongin C and 10 μM ryanodine) ($n = 12$ independent experiments). (**C** and **D**) Insulin secretion was measured by ELISA assay, normalized to microgram protein concentration, and expressed as stimulation index in (C) INS-1E cells treated as in (B) ($n = 5$ independent experiments) and (D) murine islets cultured for 48 hours under glucotoxic (25 mM glucose) or control glucose (5.5 mM) conditions and then treated as in (B) ($n = 5$ independent experiments). (**E**) Calcium fluxes were evaluated as in (A), with INS-1E cells incubated in KRBH buffer without calcium before the incubation with 25 mM glucose KRBH buffer ($n = 12$ independent experiments). (**F**) INS-1E cells were treated as in (E), and insulin secretion was measured as in (C) ($n = 6$ independent experiments). Data are represented as mean ± SD; $^*P < 0.05$ and $^{***}P < 0.001$. (A, B, and E) Statistical analysis was two-way ANOVA with Tukey's post hoc tests. (C, D, and F) Statistical analysis was one-way ANOVA with Sidak's post hoc test.

extracellular calcium influx and is tightly coupled to GSIS (*37*–*40*). While we confirmed that INS-1E cells exposed to high glucose had reduced Cav1.2 protein levels, treatment with irisin did not restore Cav1.2 expression (fig. S3B), suggesting that its ability to enhance cytosolic calcium may be independent of this plasma membrane channel. In addition to calcium influx from the extracellular space, multiple membrane-bound organelles, including the nucleus, ER, mitochondria, Golgi, and various vesicles and granules, contribute to intracellular calcium (*41*). Since irisin was recently shown to promote calcium release form the ER in vascular smooth muscle cells (*34*), we hypothesized that irisin could restore acute glucose-induced cytosolic calcium influx by stimulating calcium mobilization from the ER. To test this hypothesis, we incubated INS-1E cells cultured under glucotoxic conditions in the presence or absence of inhibitors of the ryanodine receptor (RyR) and inositol-1,4,5-trisphosphate receptor (IP3R). These receptors, located on the ER membrane (*41*), mediate calcium release from the ER, and we used their inhibition to block ER-dependent calcium flux. When we pretreated INS-1E cells with high-dose ryanodine (10 μM) and xestospongin C (1 μM), which inhibit RyR and IP3R, respectively, irisin lost the ability to restore the acute glucose-induced increase in cytosolic calcium under glucotoxic conditions (Fig. 4B). Consistently, irisin restored impaired GSIS in INS-1E cells under glucotoxic conditions, and this effect was abolished by RyR and IP3R inhibition (Fig. 4C and fig. S3C). We observed similar results in murine islets (Fig. 4D and fig. S3D). These data suggest that, under conditions of glucotoxicity, irisin restores GSIS by inducing release of calcium from the ER, regardless of the activation of AKT or CREB.

To further confirm this hypothesis, we performed similar experiments by culturing cells in calcium-free medium to prevent any entry of calcium from extracellular compartment, without affecting calcium mobilization from the ER. Under these experimental conditions, the acute glucose-induced increase in cytosolic calcium and GSIS were predictably blunted under control conditions (control cells without calcium and irisin-treated cells without calcium), while the ability of irisin to restore these responses was retained (Fig. 4, E and F, and fig. S3E).

We next investigated the mechanism by which irisin promotes calcium release from the ER under glucotoxic conditions. Since AMPK has been implicated in irisin-mediated regulation of ER calcium release in vascular smooth muscle cells (*34*), and dysregulation of the AMPK-mTORC1-S6K pathway has been linked to β cell dysfunction under chronic hyperglycemia (*31*), we hypothesized that modulation of the AMPK-mTORC1-S6K pathway may contribute to the effects of irisin on ER calcium flux in β cells. AMPK activity and mTORC1-S6K activity were determined by assessing phosphorylation of AMPKα at Thr^{172} and of the ribosomal protein S6, the downstream target of mTORC1, at $Ser^{240/244}$, respectively (*31*). As previously demonstrated (*31*), we found that AMPK phosphorylation in INS-1E cells was higher at 3 mM glucose and reduced upon acute elevation to 25 mM glucose (Fig. 5, A and B). Notably, irisin did not alter the AMPK phosphorylation profile under control conditions (Fig. 5, A and B). In contrast, glucotoxicity markedly decreased AMPK phosphorylation at both 3 and 25 mM glucose (Fig. 5, A and B), resulting in hyperphosphorylation of S6 (Fig. 5, A and C). These findings are consistent with the hyperactivation of this pathway and the associated impairment of GSIS (*31*). Irisin treatment restored AMPK phosphorylation at 3 mM glucose, reestablishing the ability of acute glucose stimulation to reduce AMPK phosphorylation under glucotoxic conditions (Fig. 5, A and B). In addition, irisin reduced glucotoxicity-induced hyperphosphorylation of S6 (Fig. 5, A and C).

To test the involvement of the AMPK-mTORC1-S6K pathway directly, we used the AMPK inhibitor compound C (30 μM; dose determined by time-course experiments; fig. S4, A and B). Because compound C can also inhibit other kinases involved in insulin secretion, such as Src and Yes (*42*), we assessed potential off-target effects. At the concentration used, compound C did not affect Tyr^{416} phosphorylation of the Src family kinase, an activating phosphorylation shared by Src and Yes (fig. S4, A and C). In addition, Tyr^{416} phosphorylation of Src was not modified by irisin (fig. S4D), thereby excluding a contribution of Src and Yes to the effects observed in our experimental conditions. Moreover, at the used concentration, compound C did not affect basal insulin secretion (fig. S4E). However, it prevented the irisin-induced restoration of AMPK and S6 phosphorylation during glucotoxicity (fig. S4, F to H).

Functionally, pretreatment of INS-1E cells with compound C abrogated the ability of irisin to restore the acute glucose-induced rise in cytosolic calcium (Fig. 5D) and to rescue GSIS (Fig. 5E and fig. S4I) under glucotoxic conditions. Collectively, these data support the concept that, under conditions of glucotoxicity, irisin promotes calcium release from the ER and recovers GSIS by restoring AMPK responsiveness to acute glucose stimulation and by reducing hyperactivation of the mTORC1-S6K pathway.

Irisin restores GSIS in human pancreatic islets from donors with T2D

Last, we investigated the effects of irisin on insulin secretion in human pancreatic islets isolated from donors without or with T2D (ND and T2D, respectively). ND islets treated with 100 nM irisin for 1 hour (Fig. 6A) showed a 1.5-fold increase in GSIS, represented as stimulation index (Fig. 6A). As expected, human pancreatic islets from subjects with T2D were characterized by a significant reduction in GSIS (Fig. 6A) when compared to ND islets, and irisin treatment restored this response (1.4-fold increase; Fig. 6A) to the levels of ND islets. The insulin secretion data of each single islet preparation is reported in Table 1. Of note, irisin stimulation for 1 hour did not modify insulin content (Table 2), suggesting that the irisin-mediated improvement in GSIS was due to a direct action of the myokine on the insulin secretory machinery.

In addition, when used for 24 hours, irisin also increased insulin content 1.6-fold (Fig. 6B) in ND islets and restored the reduced insulin content (Fig. 6B) in islets from subjects with T2D (1.7-fold increase; Fig. 6B). As already observed in the mouse model of T2D, we could not detect significant differences in apoptosis levels in islets from donors with and without T2D, treated or not with irisin (Fig. 6C). Together, these results demonstrate that irisin has the potential to restore GSIS and augment insulin content in human pancreatic islets from donors with T2D.

DISCUSSION

In this study, we show favorable effects of irisin on glucose homeostasis in a mouse model of T2D in vivo. Accordingly, irisin administration to diabetic mice reduced fasting hyperglycemia and improved glucose tolerance and GSIS. In addition, irisin reduced body weight, without inducing changes in food intake. As previously demonstrated, irisin-induced weight loss could rely on its ability to promote

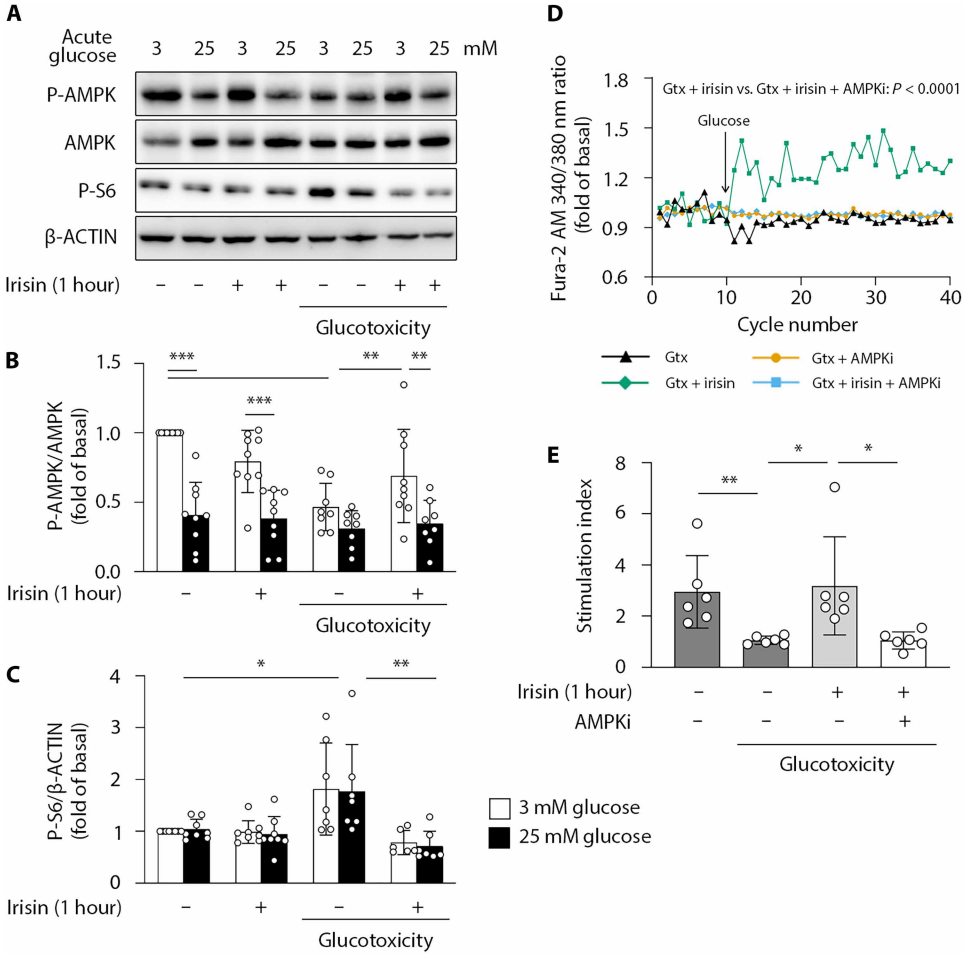

Fig. 5. Irisin restores GSIS and calcium signaling through an AMPK-dependent mechanism in INS-1E cells under glucotoxicity. (**A** to **C**) INS-1E cells were cultured for 24 hours under glucotoxic (25 mM glucose) or control glucose (11 mM) conditions and subsequently treated with 100 nM irisin for 1 hour or left untreated. Cells were then sequentially incubated in low (3 mM) and high (25 mM) glucose KRBH buffer. Protein lysates were subjected to immunoblot analysis. (A) Representative immunoblot images. Densitometric analysis of (B) P-AMPK and (C) P-S6 bands, expressed as relative optical density, corrected using (B) total AMPK or (C) β-actin, and normalized against untreated control ($n = 9$ and $n = 8$ independent experiments, respectively). (**D** and **E**) INS-1E cell were treated as in (A). As indicated, cells were pretreated with 30 μM AMPK inhibitor (AMPKi, compound C) for 30 min. (D) Intracellular calcium was measured using 1 μM Fura-2 AM fluorescence calcium reporter, and fluorescence was recorded for 10 cycles before and 30 cycles after 25 mM acute-glucose stimulation. Data are expressed as the 340/380-nm fluorescence ratio and presented as fold of basal fluorescence ($n = 8$ independent experiments). (E) Insulin concentrations in KRBH buffer were measured by ELISA assay. Secretion was normalized to microgram protein concentration and was expressed as stimulation index (25/3 mM glucose GSIS) ($n = 6$ independent experiments). Data are represented as mean ± SD; $^{*}P < 0.05$, $^{**}P < 0.01$, and $^{***}P < 0.001$. (B to D) Statistical test was two-way ANOVA with Sidak's and/or Tukey's post hoc tests. (E) Statistical test was one-way ANOVA with Sidak's post hoc test. Gtx, glucotoxicity.

white adipose tissue browning, thermogenesis, and increase in energy consumption (*43*, *44*). Consistently, we have observed that irisin administration to diabetic mice up-regulated the mRNA expression levels of browning-related genes in gonadal adipose tissue. Since irisin was not able to restore insulin sensitivity in diabetic mice, we suggest that its ability to ameliorate glycemic control may be due to enhanced insulin secretion rather than improved insulin resistance. This observation disagrees with previous studies demonstrating the ability of irisin to reduce insulin resistance in different mouse model of diabetes (*26*, *45*, *46*). However, it should be noted that in our study, we assessed insulin sensitivity using the Matsuda and HOMA-IR indexes, which both incorporate fasting insulin levels into their calculation. The irisin-induced increase in fasting insulin levels could mask subtle irisin-induced improvements in insulin sensitivity in diabetic mice, and this represents a key methodological difference from the cited studies. In two of them (*45*, *46*), insulin sensitivity was evaluated using the insulin tolerance test, which provides a more direct assessment of insulin resistance rather than a derived index. In another study (*26*), HOMA-IR was used; however, unlike in our study, diabetic mice were hyperinsulinemic, suggesting an early stage of diabetes in which β cells could still compensate for HFD-induced insulin resistance.

In addition, irisin reversed the alteration of pancreatic islet architecture in diabetic mice, by increasing islet mean area, β cell area, and insulin content while reducing α cell area, in line with previous studies in in vivo mouse model of T2D (*26*, *28*–*30*). However, in contrast to two previous reports (*29*, *47*), we did not detect differences in apoptosis levels among islets from control, diabetic, or irisin-treated diabetic mice. This discrepancy may be explained by the rapid clearance of

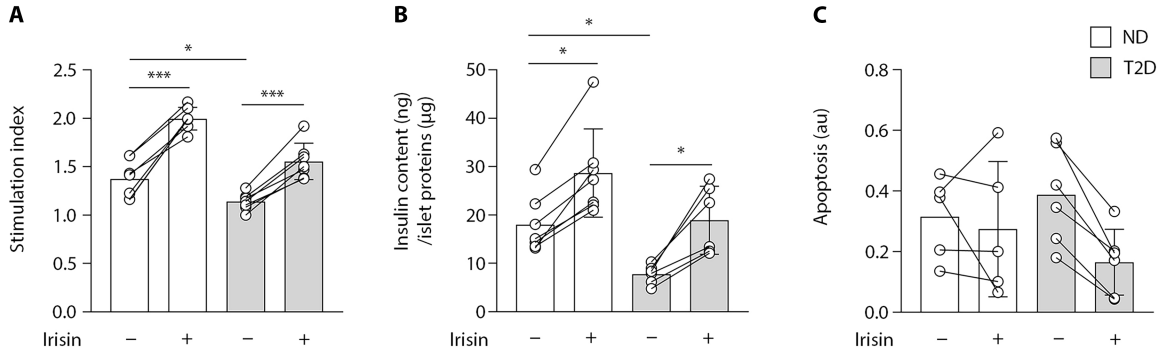

Fig. 6. Irisin restores insulin content and GSIS without affecting apoptosis in human pancreatic islets from T2D donors. (**A**) Human pancreatic islets were isolated from four donors without diabetes (ND; $n = 7$ from preparation nos. 1 to 3 and 20) and seven donors with T2D ($n = 7$ from preparation nos. 7 to 10, 16, 19, and 24). ND and T2D islets were treated with 100 nM irisin for 1 hour and then sequentially cultured with low (2.8 mM) and high (16.8 mM) glucose KRBH buffer. Insulin concentrations in KRBH buffer were measured by ELISA assay. Secretion was normalized to insulin content and expressed as stimulation index (16.8/2.8 mM glucose GSIS). (**B**) Human pancreatic islets were isolated from seven donors without diabetes (ND; $n = 7$ from preparation nos. 1 to 3, 18, and 20 to 22) and six donors with T2D ($n = 6$ from preparation nos. 11 to 13, 17, 19, and 23). ND and T2D islets were treated with 100 nM irisin for 24 hours. Insulin content (nanograms) was evaluated by ELISA assay and normalized to microgram islet protein concentration. (**C**) Human pancreatic islets were isolated from five donors without diabetes (ND; $n = 5$ from preparation nos. 1 to 3, 20, and 21) and six donors with T2D ($n = 6$ from preparation nos. 11 to 14, 17, and 19). ND and T2D islets were treated with 100 nM irisin for 24 hours. Apoptosis levels were evaluated by measuring cytoplasmic oligonucleosomes with an ELISA assay. Data are presented as mean ± SD; $^*P < 0.05$ and $^{***}P < 0.001$. Statistical test was one-way ANOVA with Sidak's post hoc test.

Table 1. Single patients' data—Insulin secretion.

	Insulin secretion (ng/ng insulin content per hour)			
	Basal		100 nM irisin 1 hour	
Preparation no.	2.8 mM Glu	16.8 mM Glu	2.8 mM Glu	16.8 mM Glu
1, ND	0.0069	0.0098	0.0071	0.0128
2, ND, n1	0.0181	0.0292	0.0178	0.0386
2, ND, n2	0.0181	0.0292	0.0172	0.0362
3, ND, n1	0.0185	0.0262	0.0259	0.0497
3, ND, n2	0.0176	0.0205	0.0211	0.0419
3, ND, n3	0.0177	0.0205	0.0208	0.0414
20, ND	0.0633	0.0775	0.0764	0.1523
7, T2D	0.0097	0.0115	0.0098	0.0160
8, T2D	0.0295	0.0346	0.0195	0.0287
9, T2D	0.0070	0.0080	0.0072	0.0116
10, T2D	0.0599	0.0649	0.0752	0.1040
16, T2D	0.0020	0.0020	0.0022	0.0032
19, T2D	0.0360	0.0398	0.0310	0.0426
24, T2D	0.0638	0.0816	0.0584	0.1120

Table 2. Single patients' data—Insulin content.

	Insulin content (ng/µg islet protein)	
Preparation no.	Basal	100 nM irisin 1 hour
1, ND	14.58	14.50
2, ND	16.55	16.47
3, ND	17.31	17.32
20, ND	14.63	14.95
7, T2D	8.26	8.25
8, T2D	9.82	9.80
9, T2D	7.14	6.90
10, T2D	12.18	12.12
16, T2D	15.23	15.76
19, T2D	8.05	7.74
24, T2D	12.38	12.50

apoptotic cells in vivo (*48*), as immunofluorescence analyses in our study were performed 25 days after STZ-induced apoptosis, when apoptotic cells were likely no longer detectable. Moreover, in previous studies, mice were fed a HFD without STZ injection, which may account for the observed differences. On the other hand, we found that irisin induced a 9-fold and 4.5-fold increase in β cell proliferation rate compared to control and vehicle-treated diabetic mice, respectively, mirroring the proliferative effects of this myokine shown in islets of healthy mice (*23*) and rodent β cell lines (*24*). This suggests that the ability of irisin to restore the β cell area and overall insulin secretory capacity may be due to increased β cell expansion even following the detrimental effects of excess fats and STZ injection. Of note, we found that the effect size of irisin on β cell area, insulin content, and β cell proliferation in diabetic mice was larger than previously observed in healthy control mice (*23*) (β cell area: 1.5-fold increase in diabetic mice versus 1.1-fold increase in control mice; insulin content: 1.6-fold increase in diabetic mice versus 1.3-fold increase in control mice; β cell proliferation: 4.3-fold increase in diabetic mice versus 2.5-fold increase in control mice), suggesting that irisin's effects could be particularly evident in a pathological context. An increase in the proliferation rate was apparent also in the exocrine pancreas, potentially raising the issue of whether irisin may trigger tumorigenesis. However, this effect appears to be due to the action of HFD rather than irisin. Accordingly, in our previous study (*23*), we did not observe proliferation in the exocrine pancreas in control healthy mice treated with irisin. Irisin has been previously reported

to exert antiproliferative and antineoplastic effects in several cell lines of pancreatic cancer (*49*, *50*).

In addition, we demonstrate that irisin restores insulin content and improves GSIS in human T2D islets, typically characterized by impaired insulin content and secretion, in the absence of significant changes in apoptosis levels. Similarly to human pancreatic islets and diabetic mice, irisin was able to restore the impaired GSIS in both INS-1E cells and murine pancreatic islets cultured under glucotoxic conditions to mimic diabetes (i.e., 25 mM glucose for 24 and 48 hours, respectively), while it did not modify apoptosis levels. However, while in previous studies demonstrating an antiapoptotic effect of irisin on pancreatic β cells irisin stimulation preceded or occurred simultaneously with the cytotoxic stimulus (*23*, *25*, *29*, *47*), in this study, we exposed diabetic mice, human pancreatic islets, and INS-1E cells to irisin after the cytotoxic damage had already occurred. Together, these results indicate that irisin can both prevent and restore glucotoxicity-induced loss of β cell function and rescue the reduced β cell mass by promoting β cell proliferation, while it can prevent but not restore glucotoxicity-induced β cell apoptosis.

We have previously shown that the ability of irisin to enhance GSIS in INS-1E cells is mediated by the irisin-induced activation of PKA/CREB (*23*). In the current study, we found that irisin cannot promote CREB or AKT phosphorylation in INS-1E cells exposed to a glucotoxic milieu, suggesting the existence of alternative mechanisms by which the myokine restores GSIS. In pancreatic β cells, GSIS is regulated by multiple drivers, comprising elevations in intracellular calcium (*41*). In INS-1E cells, irisin restored the acute glucose-induced increase in cytosolic calcium levels that was abrogated in the presence of glucotoxicity, suggesting that, in the presence of chronically elevated glucose, irisin may directly regulate the calcium fluxes and insulin secretory machinery, independently of PKA/CREB. The loss of acute glucose-induced increase in cytosolic calcium levels under glucotoxic conditions may depend on two reasons. First, calcium levels may be basally elevated following glucotoxicity, attenuating further increases in cytosolic calcium in response to acute secretory stimuli (*36*). However, in our experiments, glucotoxicity increased basal cytosolic calcium after 48 hours, while our experiments were carried out at 24 hours. Second, glucotoxicity reduced the protein expression of L-VGCC Cav1.2 in INS-1E cells, which, under physiological conditions, is the main responsible for the acute glucose-induced increase in cytosolic calcium (*37*–*40*) and is coupled to GSIS (*37*, *51*). Cav1.2 is reportedly reduced also in pancreatic islets from Zucker diabetic fatty rats and murine islets exposed to chronically elevated glucose (*37*, *38*). Nevertheless, we found that irisin did not restore Cav1.2 protein levels, indicating that its ability to restore cytosolic calcium is independent of this mechanism. Thus, we focused on intracellular calcium stores and found that irisin restored GSIS by promoting calcium mobilization from the ER, as inhibition of IP3R and RyR, the main receptors mediating ER calcium release, abolished the irisin-induced enhancement of both the acute glucose-induced rise in cytosolic calcium levels and GSIS. Accordingly, culturing cells in calcium-free medium to prevent the entry of extracellular calcium, leaving intracellular calcium stores intact, did not affect the restorative effects of irisin on cytosolic calcium responses and GSIS under conditions of glucotoxicity. It should be noted that also GLP-1 potentiates GSIS in part via the mobilization of intracellular calcium from ER (*35*). Last, to gain insight on the mechanism through which irisin promotes calcium release from the ER under glucotoxicity, we focused on AMPK (*31*, *34*). Irisin-based interventions have gained attention for their potential to modulate the AMPK pathway in various diseases, including diabetes (*33*). In addition, in vascular smooth muscle cells, it was recently shown that irisin suppresses calcium release from ER through the activation of AMPK (*34*), suggesting that AMPK activation may act as a brake on the release of calcium from the ER.

AMPK activity in pancreatic β cells is tightly regulated by glucose. Most previously published studies report that GSIS is associated with a reduction in AMPK activity and that acute glucose-mediated inhibition of AMPK represents a critical step in the glucose-triggered pathway that initiates insulin secretion (*31*, *52*). Furthermore, AMPK signaling has been reported to be constitutively down-regulated in pancreatic islets from individuals with T2D, rendering it unresponsive to glucose stimulation (*31*, *52*). In addition, AMPK acts as a key upstream negative regulator of mTORC1, a central integrator of metabolic cues that coordinates cell growth, proliferation, and survival (*53*). While tightly controlled mTORC1 signaling is required to sustain β cell mass and adaptive responses to metabolic demand, persistent and unrestrained activation appears to shift this pathway from adaptive to maladaptive. Accumulating evidence indicates that chronic mTORC1 hyperactivation contributes to β cell dysfunction in diabetes (*32*). Enhanced mTORC1 activity has been consistently observed in human and mouse islets and β cell lines exposed to high glucose, as well as in islets from multiple murine models of T2D and individuals with T2D (*54*–*57*). Consistent with these observations, we found that under control conditions, AMPK was active at 3 mM glucose and was inhibited by an acute glucose elevation to 25 mM. In contrast, under glucotoxic conditions, AMPK activity was markedly reduced at both low and high glucose concentrations. The persistent AMPK inhibition was associated with sustained mTORC1-S6K hyperactivation, as evidenced by increased phosphorylation of its downstream effector S6, in agreement with previous reports in INS-1 cells and diabetic murine islets (*31*). In the presence of glucotoxicity, irisin restored AMPK activation at 3 mM glucose and restrained the ability of acute glucose stimulation to appropriately inhibit AMPK activity. Rebalancing AMPK signaling was accompanied by attenuation of mTORC1-S6K pathway hyperactivation, ultimately favoring calcium release from the ER and GSIS. Accordingly, in INS-1E cells cultured under glucotoxic conditions, the pretreatment with compound C (an AMPK inhibitor) abolished the ability of irisin to attenuate mTORC1-S6K signaling, restore the acute glucose-induced increase in cytosolic calcium, and ameliorate GSIS. These findings are consistent with a mechanism involving the restoration of AMPK-mTORC1-S6K signaling responsiveness by irisin. Notably, short-term pharmacological inhibition of the mTORC1-S6K axis, similar to that induced by irisin, has been shown to partially restore insulin secretory capacity in diabetic human β cells (*31*, *57*), further supporting a causal link between excessive activation of mTORC1 signaling and β cell failure. Nevertheless, an apparent discrepancy may be perceived, as AMPK activation has also been reported to potentiate insulin secretion in response to glucose and other secretagogues, while prolonged activation can be deleterious for β cell function (*52*). Enhanced insulin secretion, however, occurs only at pharmacological levels of AMPK activation (*52*). Our data indicate that irisin does not act as a pharmacological AMPK activator, as it does not affect AMPK phosphorylation under control conditions. Rather, under glucotoxic conditions, irisin restores AMPK phosphorylation at 3 mM glucose to control levels without inducing its supraphysiological activation and thus without altering basal insulin secretion in vitro. Consistently, in our previously published study in normoglycemic mice (*23*), irisin

administration did not modify basal insulin secretion, in agreement with our in vitro results. Differently, in this study, irisin also increased basal insulin levels in diabetic mice under high-glucose conditions.

In previous studies, irisin was found to ameliorate β cell function and survival and to protect β cell lines and rodent islets from glucolipotoxicity-induced apoptosis and nondiabetic human islets from palmitate-induced apoptosis (*23*–*25*). However, pathophysiological processes occurring in the pancreatic islets of diabetic mice or subjects with T2D (*1*) are not always replicable in β cell lines or human/rodent pancreatic islets exposed to dysmetabolic conditions ex vivo. In this study, we show the insulin secretagogue action of irisin in an experimental model of T2D as well as in pancreatic islets from patients with T2D. In addition, we demonstrate that irisin can also restore islet architecture in diabetic mice.

These results endorse the possibility to use irisin as a tool to rescue the functional loss of pancreatic islets occurring in the disease condition. Expectedly, the effects of irisin mirror those of GLP-1 and its analogs, since numerous ex vivo studies have demonstrated that exendin-4 can improve insulin secretion in human pancreatic islets from patients with T2D with an effect of approximately the same magnitude as that seen in this study with irisin (*58*). GLP-1 receptor agonists share similar intracellular pathways with irisin in pancreatic β cells (*9*) and have the same potential to restore the human pancreatic β cell functional mass in T2D (*1*). However, here, we could also unveil the interesting bimodal properties of irisin to enhance GSIS through different mechanisms in physiological and dysmetabolic conditions, respectively. Under control conditions, irisin promotes GSIS through the activation of PKA/CREB, as previously noted (*23*), while in the presence of glucotoxicity and impaired GSIS, irisin restores GSIS by mobilizing calcium stores directly from the ER through an AMPK-mTORC1-S6K–dependent mechanism and independently of PKA/CREB (Fig. 7).

Although our findings provide compelling evidence for the beneficial effects of irisin on β cell function and islet architecture in diabetic models, several limitations should be acknowledged. First, we conducted most experiments in mice or ex vivo systems, which may not fully replicate the complexity and heterogeneity of human T2D. Moreover, the duration of irisin exposure and use of STZ-induced diabetes may not capture long-term disease dynamics or alternative pathogenic mechanisms. Mechanistically, while we identified AMPK-dependent ER calcium mobilization as a key pathway under glucotoxicity, the upstream receptors and signaling events mediating irisin's actions remain incompletely defined. In addition, although major off-target effects of compound C were excluded, the broad spectrum of action of this inhibitor may still represent a potential limitation. To move toward clinical application, future studies should include chronic administration models, assessment across diverse T2D etiologies, identification of irisin's receptor in pancreatic β cells, and controlled trials in human subjects to determine efficacy, pharmacokinetics, and safety. Only through these additional steps will it be possible to validate the therapeutic potential of irisin and its feasibility as an intervention to restore β cell function in T2D.

MATERIALS AND METHODS

Animals

Animal experiments were conducted after obtaining approval from the Ethics Committee of the Genetic Research Center "Gaetano Salvatore," Biogem, Ariano Irpino, Italy, in accordance with the *NIH Guide for the Care and Use of Laboratory Animals*, Eighth Edition (2011) and the regulations established in Italy and the EU for animal experiments (study approval number: 392/2018-PR). Six-week-old male C57Bl/6J mice ($n = 8$) were fed a HFD (60% of energy deriving from fat; formulation given in table S2) for 89 days and, on day 64, intraperitoneally injected with STZ (100 mg/kg; from Sigma-Aldrich Inc., St. Louis, MO, USA) dissolved in 0.01 M citrate buffer (pH 4.5) to induce diabetes. Combining use of a HFD with a single injection of low-dose STZ is a suitable strategy to induce T2D in C57Bl/6 mice (*59*–*61*) (further details are given in Supplementary Materials and Methods). Animals with glycemia >250 mg/dl were considered diabetic. Type 1 diabetes was ruled out on the basis of multiple lines of evidence. Following STZ injection, mice did not exhibit weight loss typically associated with type 1 diabetes induction (fig. S5). In addition, they maintained adequate insulin levels both in circulation and within pancreatic islets (Figs. 1C and 2, B and F, respectively), and they showed a partially preserved response to glucose challenge during the IPGTT (Fig. 1G). Starting on day 75, HFD/STZ mice were randomized into two groups with equal metabolic characteristics at baseline (table S1) and intraperitoneally injected with irisin (0.5 μg/g; $n = 4$) or vehicle ($n = 4$) daily for 14 days. To minimize cage and litter effects, the two groups of HFD/STZ mice were cohoused in the same cage under identical environmental conditions. Control mice ($n = 4$) were fed a SD (formulation given in table S3), received only 0.01 M citrate buffer (pH 4.5) on day 64 and were daily injected with vehicle [1× phosphate-buffered saline (PBS)], starting on day 75, for 14 days (fig. S1A). Mice and diets were purchased from Charles River Laboratories (Calco, Lecco, Italy). Irisin was purchased from AdipoGen SA (Liestal, Switzerland; catalog no. AG-40B-0103-C010). The irisin dose used in this study was selected on the basis of our previous experimental findings (*23*) and has been identified as the optimal therapeutic dose in animal models according to a recent systematic review of the literature (*62*). Fasting glycemia, insulinemia, and body weight were measured throughout the study. Food intake was recorded daily starting from the time of irisin administration by subtracting the amount of feed leftovers from the daily amount given. Matsuda index and HOMA-IR index for mice were calculated as previously suggested (equation is provided in Supplementary Materials and Methods) (*63*). On the last day of the study, IPGTT [20% glucose (2 g glucose/kg body weight)] was carried out, then animals were sacrificed, and pancreases and gonadal adipose tissue were collected. Glycemia was measured in the tail-tip blood samples by a commercial glucometer. Fasting insulin levels were measured by Ultrasensitive Mouse Insulin ELISA (enzyme-linked immunosorbent assay; Mercodia AB, Sylveniusgatan, Uppsala, Sweden; catalog no. 10-1249-01). Insulin levels during IPGTT were measured by Mouse Insulin ELISA (Mercodia AB; catalog no. 10-1247-01; more details are given in Supplementary Materials and Methods).

Immunofluorescence and islet morphometry

For immunofluorescence studies, pancreases were resected immediately after death and fixed in 4% paraformaldehyde in 1× PBS overnight at 4°C and then embedded in paraffin blocks after an ethanol wash. Embedded tissues were sliced into 4-μm-thick sections and deparaffinized with a series of xylene and ethanol washings. Antigen retrieval was performed with sodium citrate buffer followed by microwave heating. Sections were permeabilized and incubated with primary antibodies against insulin, glucagon, Ki-67, or cleaved caspase-3 overnight at 4°C, followed by fluorophore-conjugated secondary antibody for 1 hour at room temperature. A list of the

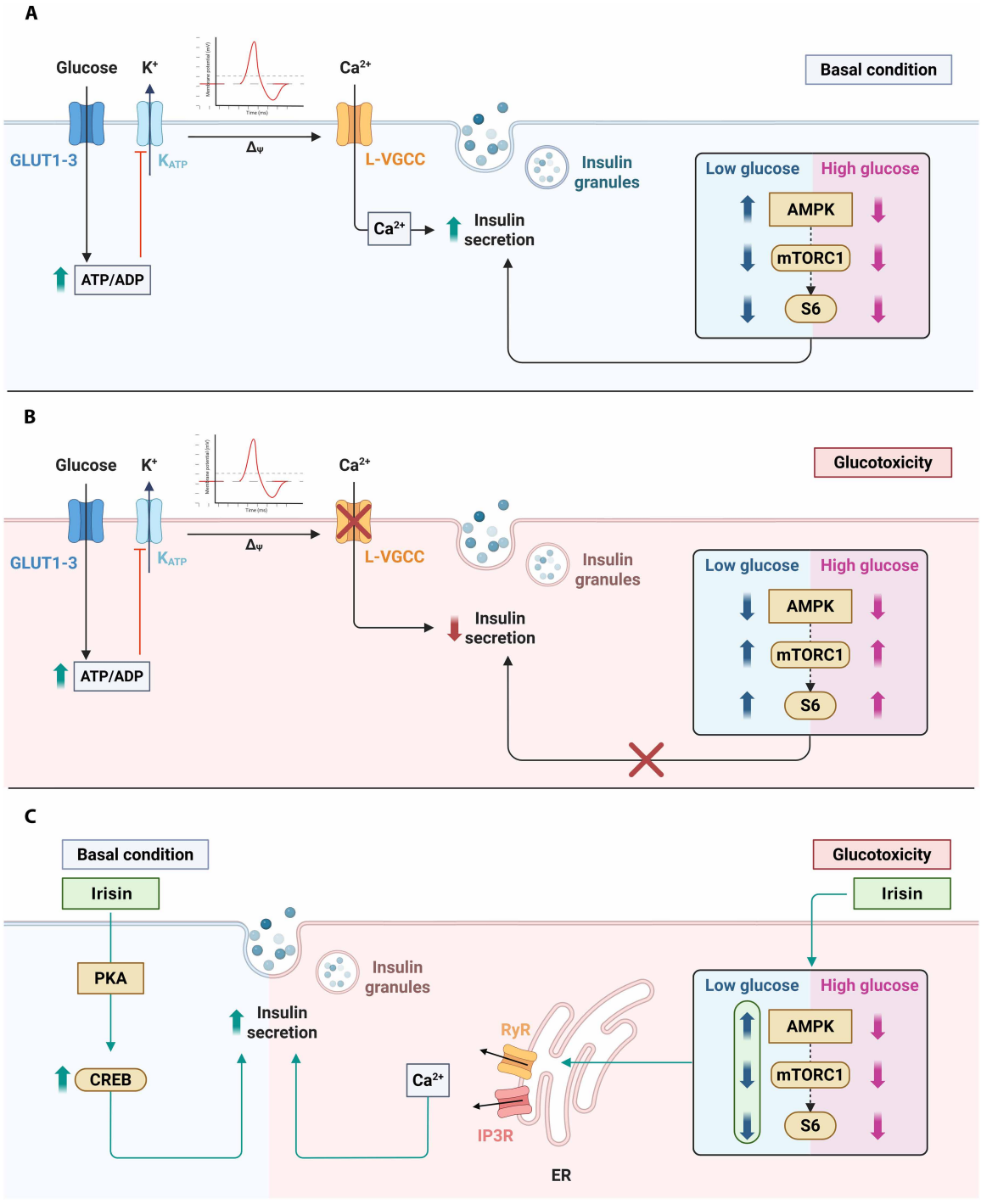

Fig. 7. Proposed mechanisms through which irisin may restore GSIS. (**A**) In nondiabetic pancreatic β cells, under basal conditions, glucose uptake via glucose transporters (GLUT1, GLUT2, or GLUT3), followed by its metabolism, increases intracellular adenosine triphosphate (ATP) levels. The resulting rise in the ATP/adenosine diphosphate (ADP) ratio promotes closure of ATP-sensitive K^+ (K_{ATP}) channels, leading to plasma membrane depolarization, opening of L-VGCCs, Ca^{2+} influx, and subsequent exocytosis of insulin granules. The AMPK-mTORC1-ribosomal protein S6 (S6) signaling axis also contributes to the regulation of GSIS. (**B**) Under glucotoxic conditions, reduced L-VGCC expression limits cytosolic Ca^{2+} influx and impairs GSIS. In addition, glucotoxicity suppresses AMPK phosphorylation and induces sustained hyperactivation of the mTORC1-S6 pathway. This aberrant signaling disrupts insulin secretion and drives progressive β cell dysfunction. (**C**) Left: Under basal conditions, irisin enhances GSIS through activation of the PKA/CREB signaling pathway. Right: In contrast, under glucotoxic conditions, irisin does not activate CREB; instead, it restores AMPK signaling, thereby attenuating hyperactivation of the mTORC1-S6 pathway. This rebalancing promotes Ca^{2+} mobilization from ER stores via IP3Rs and RyR, ultimately restoring GSIS. Created in BioRender.com. Marrano, N. (2026) https://BioRender.com/aejhbc1.

antibodies used is shown in table S4. Apoptosis was measured by using the Cell Death Detection ELISA^{PLUS} kit and In Situ Cell Death Detection Kit, TMR red (Roche Biochemicals, Indianapolis, IN, USA) according to the manufacturer's instructions. To visualize, nuclei cells were stained with 4′,6-diamidino-2-phenylindole (DAPI; 1:1000 dilution; Sigma-Aldrich). Pictures were acquired on a Nikon ECLIPSE Ti-S fluorescence microscope (Nikon, Minato, Tokyo, Japan). Buffer compositions are given in Supplementary Materials and Methods. Approximately 40 islets per experimental condition were analyzed. Islets area measurement was performed with ImageJ software, using the "freehand selections" and the "measure" tools (*64*). The β and α cell area was measured as insulin- and glucagon-positive cell area, respectively, and normalized against the total islet area, as previously performed (*65*). Insulin content was measured as intensity of insulin staining and normalized against total islet area. Cells double positive to insulin/Ki-67 or insulin/terminal deoxynucleotidyl transferase–mediated deoxyuridine triphosphate nick end labeling or cleaved caspase-3 staining were considered proliferating or apoptotic β cells, respectively. All these parameters were measured using commercial imaging software (CellProfiler).

Cell culture

Rat insulin–secreting INS-1E cells (RRID:CVCL_0351) were cultured in a 5% CO_2 atmosphere at 37°C in RPMI 1640 medium containing 11 mM glucose and adequately supplemented (a detailed composition is provided in Supplementary Materials and Methods). INS-1E cells were treated with 100 nM irisin at the indicated times [selected on the basis of dose-response studies performed in our previous study (*23*)]. As indicated, INS-1E cells were cultured under glucotoxic conditions (25 mM glucose) for 24 hours to mimic hyperglycemia. The RyR inhibitor, ryanodine (10 μM), the IP3R inhibitor, xestospongin C (1 μM), and the AMPK inhibitor, compound C (30 μM) (all from Calbiochem, Merck Millipore, Darmstadt, Germany) were added 30 min before irisin.

Pancreatic islet isolation and culture

Isolated human islets were obtained from pancreases or pancreatic biopsies of 10 subjects without diabetes and 14 patients with T2D with the approval of the Ethics Committees of the University Hospital Policlinico of Bari (study approval number: 5316, approved on 29 November 2017, with amendments on 17 October 2018 and 17 May 2023). Informed consent was obtained from each donor patient before the collection of pancreatic biopsies. Human islets were also obtained from the Islet Cell Laboratory of the University of Pisa, Pisa, Italy, the Diabetes Research Institute, IRCCS San Raffaele Hospital, Milan, Italy or purchased from PRODO Laboratories Inc. (Aliso Viejo, CA). Pancreatic biopsies were from patients undergoing duodeno-cefalo pancreatectomy for Vater's ampulla tumors at the Division of General Surgery of the Polyclinic Hospital of Bari (Bari, Italy) or at IRCCS "Saverio De Bellis" (Castellana Grotte, Bari, Italy). The characteristics of islet donors and islet preparations are reported in table S5.

Murine islets were isolated from 8-week-old male C57Bl/6J mice ($n = 30$). Isolation was achieved by collagenase digestion and density gradient purification, as previously detailed (*23*, *66*). Isolated islets were then cultured free floating at 37°C in suitable culture medium (a detailed composition is provided in Supplementary Materials and Methods), either with or without the addition of 100 nM irisin (AdipoGen; catalog no. AG-40B-0103-C010), at the indicated times. The selected dose was based on the results of our previous study (*23*). As indicated, murine islets were cultured under glucotoxic conditions (25 mM glucose) for 48 hours to mimic hyperglycemia. Ryanodine (10 μM) and xestospongin C (1 μM) were added 30 min before irisin.

Immunoblotting

For protein analysis, INS-1E cells were harvested and homogenized in protein lysis buffer (a detailed composition is provided in Supplementary Materials and Methods). Protein concentration was determined using the Bradford assay (Bio-Rad, Hercules, CA, USA). Equal amounts of protein were separated by SDS–polyacrylamide gel electrophoresis and blotted on polyvinylidene fluoride membranes. Membrane blocking and incubation with primary antibodies were performed with 5% skim milk in tris-buffered saline (1× TBS) with Tween 20, and then membranes were incubated with primary antibodies overnight at 4°C, followed by washing with TBS and incubating with a horseradish peroxidase–conjugated secondary antibody, for 1 hour at room temperature. Clarity Western ECL Substrate (Bio-Rad) was used for visualization of proteins with a Model 3000 VersadDoc Imaging System (Bio-Rad). The signal intensity of each protein band was then measured using Quantity One Software (Bio-Rad) and normalized to the corresponding total protein band. A list of the primary antibodies used is shown in table S6.

Insulin content and GSIS

Equal amounts of hand-picked, size-matched, isolated murine and human islets and INS-1E cells were seeded into complete medium in six-well dishes. For determination of insulin content, islets and INS-1E cells were stimulated with 100 nM irisin for 24 hours and then harvested and homogenized in nondenaturing lysis buffer (a detailed composition is provided in Supplementary Materials and Methods). For GSIS, islets and INS-1E cells were stimulated with irisin for 1 hour; then, they were incubated with low-glucose (2.8 mM for human islets and 3 mM for murine islets and INS-1E cells) Krebs-Ringer bicarbonate Hepes solution (KRBH; a detailed composition is provided in Supplementary Materials and Methods) with the addition of 100 nM irisin for 1 hour. Successively, islets and cells were cultured in low-glucose KRBH for 1 hour and then for a further hour in high-glucose KRBH (16.8 mM for human islets and 25 mM for murine islets and INS-1E cells). As indicated, the last incubation was made in KRBH without calcium with the addition of 0.1 mM EGTA (a detailed composition is provided in Supplementary Materials and Methods). The supernatant fractions were then obtained from each reaction well and frozen at −80°C for subsequent determination of insulin concentrations. Insulin levels were measured by Ultrasensitive Insulin ELISA (Mercodia AB; catalog no. 10-1132-01), Mouse Insulin ELISA (Mercodia AB; catalog no. 10-1247-01), or High Range Rat Insulin ELISA (Mercodia AB; catalog no. 10-1145-01). In human islets, insulin content was normalized to total islet protein amount as performed in previous studies, while insulin secretion was normalized to insulin content (*67*). In murine islets and INS-1E cells, insulin secretion was normalized to protein concentration as performed in previous studies (*67*, *68*).

Measurement of intracellular calcium levels

INS-1E cells were seeded into black 96-well plates and cultured for 24 hours, under basal or glucotoxic conditions. Following 1 hour of preincubation in 3 mM glucose KRBH buffer, cells were loaded with

1 μM Fura-2 AM (Sigma-Aldrich) and 0.02% F-127 (Molecular Probe, Eugene, Oregon, USA) for 30 min at 37°C. Then, cells were washed three times with 1× PBS and then incubated in 3 mM glucose KRBH buffer for 1 hour, to allow complete de-esterification of acetoxymethyl (AM) esters, together with 100 nM irisin. Wells without cells but with Fura-2 AM were used as fluorescence calibrators. Wells with cells but without Fura-2 AM were used as blank control. Fluorescence was measured for 10 cycles before and 30 cycles after 25 mM acute-glucose stimulation using a Varioskan plate reader (Thermo Fisher Scientific, Waltham, MA, USA) kept stably at 37°C. Fluorescence emission was read at 505 nm after samples were excited at both 340 and 380 nm. At the end of 10 readings of each excitation wavelength, 20 μl of 250 mM glucose solution was automatically injected to each well (final glucose concentration in the well equal to 25 mM), and the plate was shaken. Then, a further 30 readings were carried out. Raw data were exported as Microsoft Excel file. After blank subtraction, the ratio of the fluorescence at 340 and 380 nm, respectively, was calculated and presented as fold of basal fluorescence (average of the fluorescence of the first 10 cycles). Detailed fluorimeter settings are given in table S7. As indicated, cells were treated with 10 μM ryanodine and 1 μM xestospongin C or 30 μM compound C, 30 min before irisin, or cultured in KRBH buffer without calcium, just before fluorescence reading.

Statistical analysis

Sample sizes for mouse and islet experiments were based on power with GPower3.1.9.4 software calculations using previously generated data with a similar experimental protocol. Specifically, for the mouse experiments, an F test for one-way analysis of variance (ANOVA; fixed effects, omnibus) was used, with an effect size of $f = 1.127$ derived from previous data, $\alpha = 0.05$, and a desired power of 80%, resulting in an estimated sample size of four mice per group. For islet experiments, the number of independent biological replicates per condition was determined on the basis of the sample size required to detect a biologically relevant difference in GSIS in human pancreatic islets, which is the most challenging dataset for achieving statistical significance. On the basis of our previously obtained data, using an F test for one-way ANOVA (fixed effects, omnibus), with an effect size of $f = 0.838$, $\alpha = 0.05$, and a desired power of 80%, the estimated sample size was five biological replicates per condition. Human and murine islet experiments were conducted on the basis of equipment capabilities and experiment design. One-way or two-way ANOVA tests were used for statistical analysis, as appropriate. Tukey's or Sidak's post hoc analyses were performed as appropriate to identify specific differences. For all statistical tests, a P value of less than 0.05 was used to identify statistically different values. The used statistical test is indicated in the figure legends for each individual experiment. Results are available for each data panel in file S1. All values presented are means ± SD.

Supplementary Materials

The PDF file includes:

Supplementary Text
Figs. S1 to S5
Tables S1 to S7
Legend for file S1
References

Other Supplementary Material for this manuscript includes the following:

File S1

REFERENCES

1. N. Marrano, G. Biondi, A. Cignarelli, S. Perrini, L. Laviola, F. Giorgino, A. Natalicchio, Functional loss of pancreatic islets in type 2 diabetes: How can we halt it? *Metabolism* **110**, 154304 (2020).
2. U.K. prospective diabetes study 16. Overview of 6 years' therapy of type II diabetes: A progressive disease. U.K. Prospective Diabetes Study Group. *Diabetes* **44**, 1249–1258 (1995).
3. R. A. DeFronzo, R. Eldor, M. Abdul-Ghani, Pathophysiologic approach to therapy in patients with newly diagnosed type 2 diabetes. *Diabetes Care* **36**, S127–S138 (2013).
4. A. E. Butler, J. Janson, S. Bonner-Weir, R. Ritzel, R. A. Rizza, P. C. Butler, Beta-cell deficit and increased beta-cell apoptosis in humans with type 2 diabetes. *Diabetes* **52**, 102–110 (2003).
5. A. A. Christensen, M. Gannon, The Beta Cell in Type 2 Diabetes. *Curr. Diab. Rep.* **19**, 81 (2019).
6. C. Chen, C. M. Cohrs, J. Stertmann, R. Bozsak, S. Speier, Human beta cell mass and function in diabetes: Recent advances in knowledge and technologies to understand disease pathogenesis. *Mol. Metab.* **6**, 943–957 (2017).
7. I. Song, C. Muller, J. Louw, L. Bouwens, Regulating the beta cell mass as a strategy for type-2 diabetes treatment. *Curr. Drug Targets* **16**, 516–524 (2015).
8. P. Boström, J. Wu, M. P. Jedrychowski, A. Korde, L. Ye, J. C. Lo, K. A. Rasbach, E. A. Boström, J. H. Choi, J. Z. Long, S. Kajimura, M. C. Zingaretti, B. F. Vind, H. Tu, S. Cinti, K. Højlund, S. P. Gygi, B. M. Spiegelman, A PGC1-α-dependent myokine that drives brown-fat-like development of white fat and thermogenesis. *Nature* **481**, 463–468 (2012).
9. N. Marrano, G. Biondi, A. Borrelli, A. Cignarelli, S. Perrini, L. Laviola, F. Giorgino, A. Natalicchio, Irisin and incretin hormones: Similarities, differences, and implications in type 2 diabetes and obesity. *Biomolecules* **11**, 286 (2021).
10. S. Liu, F. Cui, K. Ning, Z. Wang, P. Fu, D. Wang, H. Xu, Role of irisin in physiology and pathology. *Front. Endocrinol.* **13**, 962968 (2022).
11. Y. Li, Z. Xu, Association between irisin and metabolic parameters in nondiabetic, nonobese adults: A meta-analysis. *Diabetol. Metab. Syndr.* **14**, 152 (2022).
12. K. H. Park, L. Zaichenko, M. Brinkoetter, B. Thakkar, A. Sahin-Efe, K. E. Joung, M. A. Tsoukas, E. V. Geladari, J. Y. Huh, F. Dincer, C. R. Davis, J. A. Crowell, C. S. Mantzoros, Circulating irisin in relation to insulin resistance and the metabolic syndrome. *J. Clin. Endocrinol. Metab.* **98**, 4899–4907 (2013).
13. D. D. Mitroi Sakizlian, L. Boldeanu, D. Clenciu, A. Mitrea, I. M. Vladu, A. E. Ciobanu Plasiciuc, M.-Z. Assani, D. Ciobanu, Association of circulating irisin with insulin resistance and metabolic risk markers in prediabetic and newly diagnosed type 2 diabetes patients. *Int. J. Mol. Sci.* **27**, 787 (2026).
14. A. Stengel, T. Hofmann, M. Goebel-Stengel, U. Elbelt, P. Kobelt, B. F. Klapp, Circulating levels of irisin in patients with anorexia nervosa and different stages of obesity—Correlation with body mass index. *Peptides* **39**, 125–130 (2013).
15. A. B. Crujeiras, M. A. Zulet, P. Lopez-Legarrea, R. de la Iglesia, M. Pardo, M. C. Carreira, J. A. Martínez, F. F. Casanueva, Association between circulating irisin levels and the promotion of insulin resistance during the weight maintenance period after a dietary weight-lowering program in obese patients. *Metabolism* **63**, 520–531 (2014).
16. J. Campolo, E. Corradi, A. Rizzardi, M. Parolini, C. Dellanoce, M. L. Di Guglielmo, P. Tarlarini, M. Cattaneo, M. G. Trivella, R. De Maria, Irisin and markers of metabolic derangement in non-diabetic Caucasian subjects with stage I-II obesity during early aging. *PLOS ONE* **15**, e0229152 (2020).
17. J. Y. Huh, G. Panagiotou, V. Mougios, M. Brinkoetter, M. T. Vamvini, B. E. Schneider, C. S. Mantzoros, FNDC5 and irisin in humans: I. Predictors of circulating concentrations in serum and plasma and II. mRNA expression and circulating concentrations in response to weight loss and exercise. *Metabolism* **61**, 1725–1738 (2012).
18. J. M. Moreno-Navarrete, F. Ortega, M. Serrano, E. Guerra, G. Pardo, F. Tinahones, W. Ricart, J. M. Fernández-Real, Irisin is expressed and produced by human muscle and adipose tissue in association with obesity and insulin resistance. *J. Clin. Endocrinol. Metab.* **98**, E769–E778 (2013).
19. I. Gouni-Berthold, H. K. Berthold, J. Y. Huh, R. Berman, N. Spenrath, W. Krone, C. S. Mantzoros, Effects of lipid-lowering drugs on irisin in human subjects in vivo and in human skeletal muscle cells ex vivo. *PLOS ONE* **8**, e72858 (2013).
20. R. Song, X. Zhao, D.-Q. Zhang, R. Wang, Y. Feng, Lower levels of irisin in patients with type 2 diabetes mellitus: A meta-analysis. *Diabetes Res. Clin. Pract.* **175**, 108788 (2021).
21. X.-L. Du, W.-X. Jiang, Z.-T. Lv, Lower circulating irisin level in patients with diabetes mellitus: A systematic review and meta-analysis. *Horm. Metab. Res.* **48**, 644–652 (2016).
22. J.-J. Liu, M. D. S. Wong, W. C. Toy, C. S. H. Tan, S. Liu, X. W. Ng, S. Tavintharan, C. F. Sum, S. C. Lim, Lower circulating irisin is associated with type 2 diabetes mellitus. *J. Diabetes Complications* **27**, 365–369 (2013).
23. A. Natalicchio, N. Marrano, G. Biondi, R. Spagnuolo, R. Labarbuta, I. Porreca, A. Cignarelli, M. Bugliani, P. Marchetti, S. Perrini, L. Laviola, F. Giorgino, The myokine irisin is released in response to saturated fatty acids and promotes pancreatic β-cell survival and insulin secretion. *Diabetes* **66**, 2849–2856 (2017).

24. S. Liu, F. Du, X. Li, M. Wang, R. Duan, J. Zhang, Y. Wu, Q. Zhang, Effects and underlying mechanisms of irisin on the proliferation and apoptosis of pancreatic β cells. *PLOS ONE* **12**, e0175498 (2017).
25. D. Zhang, T. Xie, P. S. Leung, Irisin ameliorates glucolipotoxicity-associated β-cell dysfunction and apoptosis via AMPK signaling and anti-inflammatory actions. *Cell. Physiol. Biochem.* **51**, 924–937 (2018).
26. T. Li, J. Yang, A. Tan, H. Chen, Irisin suppresses pancreatic β cell pyroptosis in T2DM by inhibiting the NLRP3-GSDMD pathway and activating the Nrf2-TrX/TXNIP signaling axis. *Diabetol. Metab. Syndr.* **15**, 239 (2023).
27. A. Tan, T. Li, J. Yang, J. Yu, H. Chen, Irisin attenuates pyroptosis in high glucose-induced pancreatic beta cells via the miR-133a-3p/FOXO1 axis. *Endokrynol. Pol.* **74**, 277–284 (2023).
28. A. Tan, T. Li, J. Yang, X. Li, W. Li, J. Yu, Irisin regulates integrin αvβ5/FAK/ERK to inhibit neutrophil extracellular traps formation and reduce pancreatic beta-cells pyroptosis in type 2 diabetes mellitus. *Diabetol. Metab. Syndr.* **17**, 279 (2025).
29. C. Liu, J. Zhou, Y. Xu, S. Gong, Y. Zhu, H. Zhang, Y. Dong, B. Zhao, X. Li, Irisin ameliorates oxidative stress-induced injury in pancreatic beta-cells by inhibiting Txnip and inducing Stat3-Trx2 pathway activation. *Oxid. Med. Cell. Longev.* **2022**, 4674215 (2022).
30. J. Yang, A. Tan, T. Li, H. Chen, Irisin alleviates the pyroptosis of β cells in T2DM by inhibiting NLRP3 inflammasome through regulating miR-19b-3p/SOCS3/STAT3 axis mediated autophagy. *IUBMB Life* **76**, 1264–1278 (2024).
31. E. Haythorne, M. Lloyd, J. Walsby-Tickle, A. I. Tarasov, J. Sandbrink, I. Portillo, R. T. Exposito, G. Sachse, M. Cyranka, M. Rohm, P. Rorsman, J. McCullagh, F. M. Ashcroft, Altered glycolysis triggers impaired mitochondrial metabolism and mTORC1 activation in diabetic β-cells. *Nat. Commun.* **13**, 6754 (2022).
32. A. Ardestani, B. Lupse, Y. Kido, G. Leibowitz, K. Maedler, mTORC1 signaling: A double-edged sword in diabetic β cells. *Cell Metab.* **27**, 314–331 (2018).
33. L. F. Laurindo, V. D. Rodrigues, L. F. Laurindo, L. M. A. Cherain, E. P. de Lima, B. L. Boaro, J. da Silva Camarinha Oliveira, E. F. B. Chagas, V. C. S. Catharin, J. F. Dos Santos Haber, P. C. Dos Santos Bueno, R. Direito, S. M. Barbalho, Targeting AMPK with irisin: Implications for metabolic disorders, cardiovascular health, and inflammatory conditions - A systematic review. *Life Sci.* **360**, 123230 (2025).
34. R. L. Li, C. L. Zhuo, X. Yan, H. Li, L. Lin, L. Y. Li, Q. Jiang, D. Zhang, X. M. Wang, L. L. Liu, W. J. Huang, Y. L. Wang, X. Y. Li, Y. Mao, Y. Chen, X. Liu, Q. C. Xu, Y. Y. Cai, X. J. Yang, H. Y. Chen, S. S. Wu, W. Jiang, Irisin attenuates vascular remodeling in hypertensive mice induced by Ang II by suppressing Ca2+−dependent endoplasmic reticulum stress in VSMCs. *Int. J. Biol. Sci.* **20**, 680–700 (2024).
35. T. Tsuboi, G. Da Silva Xavier, G. G. Holz, L. S. Jouaville, A. P. Thomas, G. A. Rutter, Glucagon-like peptide-1 mobilizes intracellular Ca2+ and stimulates mitochondrial ATP synthesis in pancreatic MIN6 β-cells. *Biochem. J.* **369**, 287–299 (2003).
36. M. Tariq, A. H. de Souza, M. Bensellam, H. Chae, M. Jaffredo, A. F. Close, J. P. Deglasse, L. R. B. Santos, A. Buemi, N. I. Mourad, A. Wojtusciszyn, M. Raoux, P. Gilon, C. Broca, J. C. Jonas, Prolonged culture of human pancreatic islets under glucotoxic conditions changes their acute beta cell calcium and insulin secretion glucose response curves from sigmoid to bell-shaped. *Diabetologia* **66**, 709–723 (2023).
37. S. N. Yang, P. O. Berggren, The role of voltage-gated calcium channels in pancreatic β-cell physiology and pathophysiology. *Endocr. Rev.* **27**, 621–676 (2006).
38. Y. Iwashima, W. Pugh, A. Depaoli, J. Takeda, S. Seino, G. Bell, K. Polonsky, Expression of calcium channel mRNAs in rat pancreatic islets and downregulation after glucose infusion. *Diabetes* **42**, 948–955 (1993).
39. M. Roe, J. Worley, Y. Tokuyama, L. Philipson, J. Sturis, J. Tang, I. Dukes, G. Bell, K. Polonsky, NIDDM is associated with loss of pancreatic beta-cell L-type Ca2+ channel activity. *Am. J. Physiol.* **270**, E133–E140 (1996).
40. C. Luan, Y. Ye, T. Singh, M. Barghouth, L. Eliasson, I. Artner, E. Zhang, E. Renström, The calcium channel subunit gamma-4 is regulated by MafA and necessary for pancreatic beta-cell specification. *Commun. Biol.* **2**, 106 (2019).
41. P. V. Sabatini, T. Speckmann, F. C. Lynn, Friend and foe: β-cell Ca^{2+} signaling and the development of diabetes. *Mol. Metb.* **21**, 1–12 (2019).
42. J. Bain, L. Plater, M. Elliott, N. Shpiro, C. J. Hastie, H. McLauchlan, I. Klevernic, J. S. C. Arthur, D. R. Alessi, P. Cohen, The selectivity of protein kinase inhibitors: A further update. *Biochem. J.* **408**, 297–315 (2007).
43. S. B. Niranjan, S. V. Belwalkar, S. Tambe, K. Venkataraman, K. A. Mookhtiar, Recombinant irisin induces weight loss in high fat DIO mice through increase in energy consumption and thermogenesis. *Biochem. Biophys. Res. Commun.* **519**, 422–429 (2019).
44. Y. Zhang, C. Xie, H. Wang, R. M. Foss, M. Clare, E. V. George, S. Li, A. Katz, H. Cheng, Y. Ding, D. Tang, W. H. Reeves, L. J. Yang, Irisin exerts dual effects on browning and adipogenesis of human white adipocytes. *Am. J. Physiol. Endocrinol. Metab.* **311**, E530–E541 (2016).
45. T.-Y. Liu, C.-X. Shi, R. Gao, H.-J. Sun, X.-Q. Xiong, L. Ding, Q. Chen, Y.-H. Li, J.-J. Wang, Y.-M. Kang, G.-Q. Zhu, Irisin inhibits hepatic gluconeogenesis and increases glycogen synthesis via the PI3K/Akt pathway in type 2 diabetic mice and hepatocytes. *Clin. Sci. (Lond.)* **129**, 839–850 (2015).
46. J. Wang, Y. T. Zhao, L. Zhang, P. M. Dubielecka, S. Zhuang, G. Qin, Y. E. Chin, S. Zhang, T. C. Zhao, Irisin improves myocardial performance and attenuates insulin resistance in spontaneous mutation (*Lepr^{db}*) mice. *Front. Pharmacol.* **11**, 769 (2020).
47. S. Zheng, N. Chen, X. Kang, Y. Hu, S. Shi, Irisin alleviates FFA induced β-cell insulin resistance and inflammatory response through activating PI3K/AKT/FOXO1 signaling pathway. *Endocrine* **75**, 740–751 (2022).
48. D. L. Eizirik, L. Pasquali, M. Cnop, Pancreatic β-cells in type 1 and type 2 diabetes mellitus: Different pathways to failure. *Nat. Rev. Endocrinol.* **16**, 349–362 (2020).
49. J. Liu, N. Song, Y. Huang, Y. Chen, Irisin inhibits pancreatic cancer cell growth via the AMPK-mTOR pathway. *Sci. Rep.* **8**, 15247 (2018).
50. D. Zhang, P. Zhang, L. Li, N. Tang, F. Huang, X. Kong, X. Tan, G. Shi, Irisin functions to inhibit malignant growth of human pancreatic cancer cells via downregulation of the PI3K/AKT signaling pathway. *Onco. Targets. Ther.* **12**, 7243–7249 (2019).
51. M. D. Nitert, C. L. F. Nagorny, A. Wendt, L. Eliasson, H. Mulder, Cav1.2 rather than Cav1.3 is coupled to glucose-stimulated insulin secretion in INS-1 832/13 cells. *J. Mol. Endocrinol.* **41**, 1–11 (2008).
52. T. Szkudelski, K. Szkudelska, The relevance of AMP-activated protein kinase in insulin-secreting β cells: A potential target for improving β cell function? *J. Physiol. Biochem.* **75**, 423–432 (2019).
53. G. Y. Liu, D. M. Sabatini, mTOR at the nexus of nutrition, growth, ageing and disease. *Nat. Rev. Mol. Cell Biol.* **21**, 183–203 (2020).
54. Q. Ni, J. Song, Y. Wang, J. Sun, J. Xie, J. Zhang, G. Ning, W. Wang, Q. Wang, Proper mTORC1 activity is required for glucose sensing and early adaptation in human pancreatic β cells. *J. Clin. Endocrinol. Metab.* **106**, e562–e572 (2021).
55. R. Jaafar, S. Tran, A. N. Shah, G. Sun, M. Valdearcos, P. Marchetti, M. Masini, A. Swisa, S. Giacometti, E. Bernal-Mizrachi, A. Matveyenko, M. Hebrok, Y. Dor, G. A. Rutter, S. K. Koliwad, A. Bhushan, mTORC1 to AMPK switching underlies β-cell metabolic plasticity during maturation and diabetes. *J. Clin. Invest.* **129**, 4124–4137 (2019).
56. E. Bachar, Y. Ariav, M. Ketzinel-Gilad, E. Cerasi, N. Kaiser, G. Leibowitz, Glucose amplifies fatty acid-induced endoplasmic reticulum stress in pancreatic beta-cells via activation of mTORC1. *PLOS ONE* **4**, e4954 (2009).
57. T. Yuan, S. Rafizadeh, K. D. D. Gorrepati, B. Lupse, J. Oberholzer, K. Maedler, A. Ardestani, Reciprocal regulation of mTOR complexes in pancreatic islets from humans with type 2 diabetes. *Diabetologia* **60**, 668–678 (2017).
58. R. Lupi, R. Mancarella, S. Del Guerra, M. Bugliani, S. Del Prato, U. Boggi, F. Mosca, F. Filipponi, P. Marchetti, Effects of exendin-4 on islets from type 2 diabetes patients. *Diabetes. Obes. Metab.* **10**, 515–519 (2008).
59. M. Kleinert, C. Clemmensen, S. M. Hofmann, M. C. Moore, S. Renner, S. C. Woods, P. Huypens, J. Beckers, M. H. de Angelis, A. Schürmann, M. Bakhti, M. Klingenspor, M. Heiman, A. D. Cherrington, M. Ristow, H. Lickert, E. Wolf, P. J. Havel, T. D. Müller, M. H. Tschöp, Animal models of obesity and diabetes mellitus. *Nat. Rev. Endocrinol.* **14**, 140–162 (2018).
60. T. Yu, M. J. Sungelo, I. J. Goldberg, H. Wang, R. H. Eckel, Streptozotocin-treated high fat fed mice: A new type 2 diabetes model used to study canagliflozin-induced alterations in lipids and lipoproteins. *Horm. Metab. Res.* **49**, 400–406 (2017).
61. J. H. Parilla, J. R. Willard, B. M. Barrow, S. Zraika, A mouse model of beta-cell dysfunction as seen in human type 2 diabetes. *J. Diabetes Res.* **2018**, 6106051 (2018).
62. F. Alzoughool, M. B. Al-Zghoul, S. Al-Nassan, L. Alanagreh, D. Mufleh, M. Atoum, The optimal therapeutic irisin dose intervention in animal model: A systematic review. *Vet. World* **13**, 2191–2196 (2020).
63. M. E. Nelson, S. Madsen, K. C. Cooke, A. M. Fritzen, I. H. Thorius, S. W. C. Masson, L. Carroll, F. C. Weiss, M. M. Seldin, M. Potter, S. L. Hocking, D. J. Fazakerley, A. E. Brandon, S. Thillainadesan, A. M. Senior, G. J. Cooney, J. Stöckli, D. E. James, Systems-level analysis of insulin action in mouse strains provides insight into tissue- and pathway-specific interactions that drive insulin resistance. *Cell Metab.* **34**, 227–239.e6 (2022).
64. L. Zhou, X. He, P. Cai, T. Li, R. Peng, J. Dang, Y. Li, H. Li, F. Huang, G. Shi, C. Xie, Y. Lu, Y. Chen, Induced regulatory T cells suppress Tc1 cells through TGF-β signaling to ameliorate STZ-induced type 1 diabetes mellitus. *Cell. Mol. Immunol.* **18**, 698–710 (2021).
65. Q. Jiang, Q. Zhao, Y. Chen, C. Ma, X. Peng, X. Wu, X. Liu, R. Wang, S. Hou, L. Kong, Y. Wan, S. Wang, Z. X. Meng, B. Cui, L. Chen, P. Li, Galectin-3 impairs calcium transients and β-cell function. *Nat. Commun.* **15**, 3682 (2024).
66. R. Lupi, F. Dotta, L. Marselli, S. Del Guerra, M. Masini, C. Santangelo, G. Patané, U. Boggi, S. Piro, M. Anello, E. Bergamini, F. Mosca, U. Di Mario, S. Del Prato, P. Marchetti, Prolonged exposure to free fatty acids has cytostatic and pro-apoptotic effects on human pancreatic islets: Evidence that beta-cell death is caspase mediated, partially dependent on ceramide pathway, and Bcl-2 regulated. *Diabetes* **51**, 1437–1442 (2002).
67. S. Gheibi, L. R. Cataldo, A. Hamilton, M. Huang, S. Kalamajski, M. Fex, H. Mulder, Reduced expression level of protein phosphatase PPM1E serves to maintain insulin secretion in type 2 diabetes. *Diabetes* **72**, 455–466 (2023).
68. L. Kong, Q. Zhao, X. Jiang, J. Hu, Q. Jiang, L. Sheng, X. Peng, S. Wang, Y. Chen, Y. Wan, S. Hou, X. Liu, C. Ma, Y. Li, L. Quan, L. Chen, B. Cui, P. Li, Trimethylamine N-oxide impairs β-cell function and glucose tolerance. *Nat. Commun.* **15**, 2526 (2024).

69. X. Hou, B. Xing, G. Zhang, H. Wu, N. Feng, Y. Li, G. Han, Serum irisin is associated with bone mineral density in postmenopausal T2DM patients complicated with osteoporosis and in mice with diabetic osteoporosis. *Curr. Protein Pept. Sci.* **24**, 355–363 (2023).
70. H. Duan, B. Ma, X. Ma, H. Wang, Z. Ni, B. Wang, X. Li, P. Jiang, M. Umar, M. Li, Anti-diabetic activity of recombinant irisin in STZ-induced insulin-deficient diabetic mice. *Int. J. Biol. Macromol.* **84**, 457–463 (2016).
71. C. Zhang, D. Zhang, H. Wang, Q. Lin, M. Li, J. Yuan, G. Gao, J. Dong, Hyperbaric oxygen treatment improves pancreatic β-cell function and hepatic gluconeogenesis in STZ-induced type-2 diabetes mellitus model mice. *Mol. Med. Rep.* **25**, 90 (2022).
72. Y.-S. Lee, D. Lee, G.-S. Park, S.-H. Ko, J. Park, Y.-K. Lee, J. Kang, Lactobacillus plantarum HAC01 ameliorates type 2 diabetes in high-fat diet and streptozotocin-induced diabetic mice in association with modulating the gut microbiota. *Food Funct.* **12**, 6363–6373 (2021).
73. W. Wang, R. D. Wu, P. Chen, X. J. Xu, X. Z. Shi, L. H. Huang, Z. L. Shao, W. Guo, Liraglutide combined with human umbilical cord mesenchymal stem cell transplantation inhibits beta-cell apoptosis via mediating the ASK1/JNK/BAX pathway in rats with type 2 diabetes. *Diabetes Metab. Res. Rev.* **36**, e3212 (2020).
74. L.-N. Chen, Q. Sun, S.-Q. Liu, H. Hu, J. Lv, W.-J. Ji, M. Wang, M.-X. Chen, J. Zhou, Erythropoietin improves glucose metabolism and pancreatic β-cell damage in experimental diabetic rats. *Mol. Med. Rep.* **12**, 5391–5398 (2025).
75. M. Fukaya, Y. Tamura, Y. Chiba, T. Tanioka, J. Mao, Y. Inoue, M. Yamada, C. Waeber, Y. Ido-Kitamura, T. Kitamura, M. Kaneki, Protective effects of a nicotinamide derivative, isonicotinamide, against streptozotocin-induced β-cell damage and diabetes in mice. *Biochem. Biophys. Res. Commun.* **442**, 92–98 (2013).
76. J. A. Engelman, L. Chen, X. Tan, K. Crosby, A. R. Guimaraes, R. Upadhyay, M. Maira, K. McNamara, S. A. Perera, Y. Song, L. R. Chirieac, R. Kaur, A. Lightbown, J. Simendinger, T. Li, R. F. Padera, C. García-Echeverría, R. Weissleder, U. Mahmood, L. C. Cantley, K.-K. Wong, Effective use of PI3K and MEK inhibitors to treat mutant Kras G12D and PIK3CA H1047R murine lung cancers. *Nat. Med.* **14**, 1351–1356 (2008).
77. B. D. Fonseca, T. Alain, L. K. Finestone, B. P. H. Huang, M. Rolfe, T. Jiang, Z. Yao, G. Hernandez, C. F. Bennett, C. G. Proud, Pharmacological and genetic evaluation of proposed roles of mitogen-activated protein kinase/extracellular signal-regulated kinase kinase (MEK), extracellular signal-regulated kinase (ERK), and p90(RSK) in the control of mTORC1 protein signaling by phorbol esters. *J. Biol. Chem.* **286**, 27111–27122 (2011).
78. E.-G. Hong, B. W. Kim, D. Y. Jung, J. H. Kim, T. Yu, W. S. Da Silva, R. H. Friedline, S. D. Bianco, S. P. Seslar, H. Wakimoto, C. I. Berul, K. S. Russell, K. W. Lee, P. R. Larsen, A. C. Bianco, J. K. Kim, Cardiac expression of human type 2 iodothyronine deiodinase increases glucose metabolism and protects against doxorubicin-induced cardiac dysfunction in male mice. *Endocrinology* **154**, 3937–3946 (2013).
79. M. A. Davis, M. R. Fairgrieve, A. D. Hartigh, O. Yakovenko, B. Duvvuri, C. Lood, W. E. Thomas, S. L. Fink, M. Gale Jr., Calpain drives pyroptotic vimentin cleavage, intermediate filament loss, and cell rupture that mediates immunostimulation. *Proc. Natl. Acad. Sci. U.S.A.* **116**, 5061–5070 (2019).
80. V. S. Marsden, L. O'Connor, L. A. O'Reilly, J. Silke, D. Metcalf, P. G. Ekert, D. C. S. Huang, F. Cecconi, K. Kuida, K. J. Tomaselli, S. Roy, D. W. Nicholson, D. L. Vaux, P. Bouillet, J. M. Adams, A. Strasser, Apoptosis initiated by Bcl-2-regulated caspase activation independently of the cytochrome c/Apaf-1/caspase-9 apoptosome. *Nature* **419**, 634–637 (2002).
81. R. E. Dolmetsch, U. Pajvani, K. Fife, J. M. Spotts, M. E. Greenberg, Signaling to the nucleus by an L-type calcium channel-calmodulin complex through the MAP kinase pathway. *Science* **294**, 333–339 (2001).
82. A. P. Kumar, S. Bhaskaran, M. Ganapathy, K. Crosby, M. D. Davis, P. Kochunov, J. Schoolfield, I.-T. Yeh, D. A. Troyer, R. Ghosh, Akt/cAMP-responsive element binding protein/cyclin D1 network: A novel target for prostate cancer inhibition in transgenic adenocarcinoma of mouse prostate model mediated by Nexrutine, a Phellodendron amurense bark extract. *Clin. Cancer Res.* **13**, 2784–2794 (2007).
83. Y. W. Chung, H. K. Kim, I. Y. Kim, M. B. Yim, P. B. Chock, Dual function of protein kinase C (PKC) in 12-O-tetradecanoylphorbol-13-acetate (TPA)-induced manganese superoxide dismutase (MnSOD) expression: Activation of CREB and FOXO3a by PKC-alpha phosphorylation and by PKC-mediated inactivation of Akt, respectively. *J. Biol. Chem.* **286**, 29681–29690 (2011).
84. B. E. Lonze, D. D. Ginty, Function and regulation of CREB family transcription factors in the nervous system. *Neuron* **35**, 605–623 (2002).

Acknowledgments: We thank P. Pontrelli and M. Lauriero (Nephrology, Dialysis and Transplantation Unit, Department of Precision and Regenerative Medicine and Ionian Area, University of Bari Aldo Moro, Bari, Italy) for technical assistance in immunofluorescence experiments. **Funding:** This work was supported by the European Union (European Social Fund, PON R&I 2014-2020, AIM 1810057) (N.M. and F.G.); the Regione Puglia Grant for "Tecnopolo per la Medicina di Precisione" D.G.R. no. 2117 of 21.11.2018 (F.G.); the "Fondazione per la Ricerca Biomedica Saverio e Isabella Cianciola" (F.G.); the Ministero dello Sviluppo Economico–2019, Bando PoC-MISE–Programma #NOACRONYM (A.N.); the Next Generation EU, in the context of the National Recovery and Resilience Plan, Investment PE8–Project Age-It: "Ageing Well in an Ageing Society" (F.G.). **Author contributions:** N.M.: Writing—original draft, conceptualization, investigation, writing—review and editing, methodology, resources, data curation, validation, formal analysis, and visualization. A.B.: Investigation and methodology. G.B.: Investigation and methodology. M.R.: Investigation and methodology. R.D.: Investigation. V.A.G.: Investigation. C.C.: Investigation. V.G.: Investigation and methodology. G.G.: Investigation and methodology. L.R.: Resources. A.S.: Visualization. L.V.: Resources. F.A.: Resources. R.N.: Resources. F.B.: Investigation, validation, and formal analysis. A.M.: Writing—review and editing and supervision. L.G.L.: Resources. P.M.: Resources. L.P.: Resources. A.C.: Visualization. S.P.: Visualization. L.L.: Supervision and visualization. F.G.: Conceptualization, writing—review and editing, funding acquisition, validation, supervision, project administration, and visualization. A.N.: Writing—original draft, conceptualization, funding acquisition, data curation, supervision, project administration, and visualization. **Competing interests:** The following approved patents are related to the present study: "Pharmacological use of a myokine capable of preserving the function and mass of pancreatic cells under dysmetabolic conditions," granted in Italy (23 April 2018, no. 102015000071015), Europe (12 January 2022, no. 3373955), the USA (17 September 2019, no. 10413596), and Hong Kong (14 February 2019, no. 19119431.5). The filing organization is the University of Bari Aldo Moro, and the inventors are F.G., A.N., and N.M. All other authors declare that they have no competing interests. **Data, code, and materials availability:** All data and code needed to evaluate and reproduce the results in the paper are present in the paper and/or the Supplementary Materials. This study did not generate new materials.

Submitted 4 December 2025
Accepted 27 April 2026
Published 5 June 2026
10.1126/sciadv.aee4804

ScienceAdvances

The myokine irisin ameliorates the secretory dysfunction of pancreatic # cells in experimental and human type 2 diabetes

Nicola Marrano, Anna Borrelli, Giuseppina Biondi, Martina Rella, Rossella D'Oria, Valentina Annamaria Genchi, Cristina Caccioppoli, Valerio Galasso, Giovanni Galluzzi, Luca Roberto, Anna Signorile, Leonardo Vincenti, Fabrizio Aquilino, Rita Nano, Federico Baruzzi, Antonio Moretti, Luigi Giovanni Lupo, Piero Marchetti, Lorenzo Piemonti, Angelo Cignarelli, Sebastio Perrini, Luigi Laviola, Francesco Giorgino, and Annalisa Natalicchio

Sci. Adv. **12** (23), eaee4804. DOI: 10.1126/sciadv.aee4804